Proc Indian Natn Sci Acad **82** No. 3 July Spl Issue 2016 pp. 581-604

DOI: 10.16943/ptinsa/2016/48469

Review Article

Tectonics and Evolution of the Himalaya

A K JAIN[1,*], S DASGUPTA[2], O N BHARGAVA[3], Md ISRAIL[4], R JAYANGONDA PERUMAL[5], R C PATEL[6], M MUKUL[7], S K PARCHA[5], V ADLAKHA[5], K K AGARWAL[8], P SINGH[5], K BHATTACHARYYA[9], N C PANT and D M BANERJEE[10]

[1]*CSIR-Central Building Research Institute Roorkee, India*
[2]*Department of Geography, Jamia Millia Islamia, New Delhi, India*
[3]*103 Sector 7, Panchkula, India*
[4]*Department of Earth Sciences, IIT Roorkee, Roorkee, India*
[5]*Wadia Institute of Himalayan Geology, Dehra Dun, India*
[6]*Department of Geophysics, Kurukshetra University, Kurukshetra, India*
[7]*Department of Earth Sciences, IIT Bombay, Powai, Mumbai, India*
[8]*Centre of Advanced Study in Geology, University of Lucknow, Lucknow, India*
[9]*Indian Institute of Science Education and Research, Kolkata, India*
[10]*Department of Geology, University of Delhi, Delhi, India*

(Received on 24 April 2016; Accepted on 28 April 2016)

During the period 2011-2015, scientific investigations in the Himalaya incorporated various geological and geophysical aspects of evolution of this mountain, including sub-surface configuration, structure and metamorphism of the Lesser Himalaya and Himalayan Metamorphic Belt, geochemistry, magmatism, stratigraphy and paleontology of the Paleo-Mesozoic Tethyan sedimentary cover, the Himalayan foreland basins, exhumation, paleoseismology and GPS measurements of convergence rates. Certain remote areas of western Arunachal Pradesh in Kameng were covered for their metamorphism and exhumation. Sm-Nd isochron plot of garnet crystals from the Lesser Himalayan Jutogh Group metamorphics provided a mean regression age of 479.7±8.5 Ma as the timing of its crystallization during an Early Ordovician tectonometamorphic event. High-resolution work on metamorphism of the Lesser and Higher Himalayan belts of Sikkim incorporating P-T-t paths and geochronology of the imbricate zones of the Main Central Thrust provided better insight into their evolution.

Keywords: India-Asia Convergence; Tectonics-Himalaya; Metamorphism; Exhumation; Paleoseismology; Geometry of Indian Plate

Introduction

After the final closure of the Neo-Tethys along the Shyok Suture Zone (SSZ) in the north and the Indus Tsangpo Suture Zones (ITSZ) towards south, continental India Plate with its Paleo-Mesozoic Tethyan sedimentary cover was remobilized into the Himalayan Metamorphic Belt (HMB); the Main Central Thrust (MCT) brought this belt over the Proterozoic-Paleozoic Lesser Himalayan (LH) sedimentary belt which, in turn, overrode the Cenozoic Sub-Himalayan (SH) belt along the Main Boundary Thrust (MBT). The latter is subsequently thrust over the Indo-Gangetic Plains (IGP) along the Main Frontal Thrust (MFT).

After late Mesozoic subduction of the Neo-Tethyan oceanic lithosphere along the SSZ and the ITSZ, Cenozoic convergence followed southward to evolve the Himalayan orogen, and produced (i) Tethyan Himalayan Sequence (THS), (ii) Himalayan Metamorphic Belt (HMB) containing Tso Morari Crystallines (TMC), Higher Himalayan Crystallines (HHC) and Lesser Himalayan Crystallines (LHC), (iii) Lesser Himalaya (LH) Sedimentary Belt, and (iv) Sub-Himalayan (SH) Cenozoic belt. Various National

*Author for Correspondence: E-mail: himalfes@gmail.com

groups investigated the **"Tectonics and evolution of the Himalaya"** individually or in collaboration with many International groups during 2011-2015. Their scientific achievements are recorded here under the following topics: (i) Tectonics, metamorphism and stratigraphy, (ii) Lesser Himalayan Sedimentary Belt: Late Precambrian/Cambrian sequences, (iii) Magmatism in the Himalaya, (iv) Evolution of Himalayan Foreland, (v) Exhumation, (vi) Paleoseismology and convergence rates, and (vii) Geometry of the Indian Plate (IP).

Tectonics, Metamorphism and Stratigraphy

Tethyan Himalayan Sequence (THS): Scattered geological information about the "Kashmir Basin" was compiled and synthesized for the evolution of this basin, which contains the Tethyan sequence ranging in age from Late Precambrian to Early Jurassic and unconformably overlying the Karewa succession of the Quaternary age (Bhargava, 2015). The Late Precambrian-Early Cambrian Hapatnar Group rests nonconformably over the Salkhala metamorphics, and is unconformably overlain by Early Ordovician-Middle Silurian Rishkobal Group, followed by Early-Middle (?) Devonian Muth Formation with a probable disconconformity. The Muth Formation is succeeded by the Lidder Group of the Devonian Wazura Formation, Tournaisian Aishmuqam (Syringothyrus Limestone), Visean-Serpukhian Ganeshpur Formation (Fenestella Shales), Asselian-Sakmarian Pindabol Formation and the post-early Artinskian Nishatbagh Formation. It is followed by ca 289 Ma Panjal Volcanics, which is overlain by the Wuchiapingian Zewan Formation and, in turn, succeeded by the Changhsingian to Late Triassic Vihi Group. Discrete events across the Permian-Triassic boundary indicate minor environmental changes prior to end-Permian crisis. Mostly, the volcanism and climatic changes rather than a bolide impact is considered as cause of the end-Permian crisis. Seismites and tsunamites are also recorded along the Permian-Triassic boundary in the Guryul section.

The pre-Panjal Volcanic sediments of Kashmir display litho- and biofacies similarities to the Spiti-Zanskar area. On the contrary, post-Panjal Volcanic sediments of Kashmir represent shallower water deposits as compared to those in the Spiti-Zanskar sector. It is suggested that the Kashmir "Basin" existed in strike continuity of the Spiti-Zanskar Basin till Early Permian. During rift-related outpouring of Panjal Volcanics the Kashmir area was sheared and brought in up-depositional dip of the Spiti-Zanskar Basin.

The Late Neoproterozoic-Early Jurassic succession was folded into a synclinorium (Bhargava, 2015). During the Quaternary a basin developed above it in which the Karewa sediments were deposited. The Kashmir Synclinorium was transported to its present position on back of the Panjal Thrust. There is approximately 35% crustal shortening in the Kashmir area related to the Himalayan Orogeny. Drilling for hydrocarbon in the Karewa sediments indicates gas shows at shallow depths containing 50% to 95% methane.

The fossiliferous Cambrian sequence of Spiti-Zanskar basins are corresponding to one another as far as the distribution of fauna is concerned. The early Cambrian successions in both the basins have more or less identical ichnofaunal assemblages (Parcha and Pandey, 2011a). Pagetids along with polymerid trilobites dominate the Spiti Basin in lower middle Cambrian (Parcha and Pandey, 2011a). Latest Middle Cambrian polymerid trilobites, *Pianspis, Neoanomocarella asiatica*, *Parablackwelderia* sp., were collected from Lejopyge acantha Zone of Guzhangian Stage (Cambrian Series 3) by Singh (2013). The fauna is correlatable with that of South China, North Korea, Kazakhastan, Uzbekistan, Siberia and Australia.

Singh *et al*. (2015) reported *Yuehsienszella* (Cambrian Series 2) trilobite from the Kunzam La Formation, Parahio Valley. The fossil occurring 237 m below the *Oryctocephalus indicus* level of Cambrian Series 3 (Stage 1), indicates a late Tsanglangpuian age (Cambrian Series 2, Stage 4) within the Kunzam La Formation and revises the lower age limit to Tsanglangpuian (Cambrian Series 2).

Virmani *et al*. (2015a) recognized five lithofacies during ichnofacies and ichnofabric analysis in which ichnofacies indices range from i1=80.5% (25.8 m), ii2=17% (5.4 m) and ii4=2.5% (0.8 m) in a 74 m exposed section at Khemengar locality. In the main Parahio Valley in a 42 m section the ichnofabric indices are ii1=37% (7.8 m), ii2=21% (8 m), ii3=40% (15.2 m) and ii4=2% (1 m). Cruziana facies, parallel

and wavy bedding, hummocky cross stratification and trough cross stratification indicate wave dominated shallow marine environment of deposition.

Singh *et al.* (2015) reported an assemblage of mineralised skeletal fossils (Small Shelly Fauna SSF) from lower part of the Kunzam La Formation comprising single-rayed or disarticulated sclerites of Chancelloriids, *Archiasterella* sp., *Chancelloria*, *Hyoliths*, ?*Cupitheca* sp.; Indeterminate *hyoliths*; *Helkieria* sp., indeterminate hyolitheminthes tubes, and are assigned to the Cambrian Series 2 (Stage 4). Hayden level 2 was precisely marked in the Kunzam La Formation on left bank of the Parahio River, and brackets stratigraphic range of key taxon *Oryctocephalus indicus*, defining the base of the Cambrian Series 3 (Stage 5) and possibly the Cambrian Series 2-Series 3 boundary interval all over the globe (Singh *et al*., in press). The FAD and LAD of *Oryctocephalus indicus* is recorded at 7.47 m and 14.61 m respectively, indicating 6.87 m stratigraphic range of this taxon in the Parahio Valley. The *Oryctocephalus indicus* zone is demarcated with precise stratigraphic range of eponymous species. The FADs of Pagetia and Kunmingaspis at 7.34 m predate the FAD of *Oryctocephalus indicus*. Pagetia ranges from Cambrian Series 2 (Stage 4) to Cambrian Series 3 (Stage 5). *Eosoptychoparia* has been recorded for the first time from the Himalaya. The base of the Cambrian Series 3 is proposed at the FAD of *Oryctocephalus indicus*.

Vermani *et al*. (2015b) collected additional new faunal elements of trilobites and ichnofossils from four sections, which led to further refinement of the existing Cambrian biostratigraphy of the Parahio valley in Spiti region.

In the Kumaon-Garhwal region earlier workers and in recent year's ichnofossils of early Cambrian age have been reported along with some fragments of trilobites (Upadhyay and Parcha, 2012).

The Muth Formation is one of the most characteristic marker horizon throughout the NW Himalaya. The presence of ichnofossils in the Muth Formation of the Spiti valley, according to Parcha and Pandey (2011b), indicates subtidal, whereas gradual maturity of quartz grains from base to top indicates deposition under high energy subtidal shallow marine environment.

A synpotic account of Devonian of Indian Plate was published in English as well as in Hindi (Bhargava and Draganits, 2015) in Planet Earth in Deep Times-a compilation of Devonian and Carboniferous.

Williams *et al*. (2012) investigated black shale from the Permian (Gungri Formation) of the Permian-Triassic boundary at Atargoo in Spiti Valley to interpret the paleoenvironmental conditions. However, original geochemical signatures are obscured by diagenesis and weathering. The Gungri Shale (Kuling Group) is unconformably capped by an iron-rich pebble-sand "ferruginous layer", which marks the Permian-Triassic boundary. High resolution analysis of the Gungri at Attargoo (~3 cm intervals) by multivariate chemometric techniques (e.g., Principal Component Analysis) revealed discrete sequence of events including transient iron-enrichments, which are attributed to euxinic depositional conditions and late diagenetic formation of siderite and regression condensation surfaces associated with pulsed transgression-regression towards the uppermost Permian.

In another more detailed paper on P/Tr boundary at Atargoo and Guling, Ghosh *et al*. (2015) interpreted global consequences of the Permian-Triassic (P-Tr) extinction along a remnant of the peri-Gondwanan shelf in Spiti Valley, which preserves trails of this environmental catastrophe in the Neo-Tethys Ocean. Detailed high-resolution sedimentary observations, trace element concentrations and C, O, Pb isotope data, framboidal pyrites and fossils of the Late Permian shale across the P-Tr boundary indicate deeper anoxic depositional environment. $\delta^{13}C_{org}$ excursions of 2.4‰ and 3.1‰ in Atargu and Guling outcrops, respectively, identify the P-Tr transition across a clayey, partly gypsiferous ferruginous layer. Sedimentological resemblance of this layer to other Neo-Tethyan sections from Trans-Caucasia and Iran indicates subaqueous oxidation of shallow marine sediments on a regional scale. LREE-enriched Late Permian shales with conspicuous Ce-Eu anomalies reflect their source from the adjacent Panjal Trap basalts (ca. 289 Ma) of Kashmir. Continental crustal Nb-Ta and Zr-Hf anomalies appear in sediments at the P-Tr boundary and prevail through the overlying Early Triassic carbonates. Original Pb isotope ratios along with an increasing Pb abundance closer to the P-Tr boundary, distinguish the volcanic source of Late

Permian shales from the continental crustal siliciclastic signature of Early Triassic carbonates. Our $\delta^{13}C_{org}$, trace element and Pb isotopes record from Spiti indicate catastrophic changes in sediment sources and facies, with effects on productivity. It is consistent with an abrupt episode of marine regression and erosional forcing observed elsewhere along northern Gondwanaland. Simultaneous eruption of Siberian volcanics and bolide impacts in Parana basin of Brazil and elsewhere, in combination, left catastrophic local to regional imprints on sea level, climate, marine anoxia and tectonic stability that connected the P-Tr crisis across terrestrial and marine realms of the peri-Gondwana region.

Chamba nappe: In the western Himalaya low grade metamorphosed Tethyan Himalayan Sequence (THS) is thrust southwestwards over the Higher Himalayan Crystalline (HHC) belt of the Chenab-Miyar valleys as the Chamba Nappe (Lahoti *et al.*, 2016). This nappe is comprised of Proterozoic-Paleo-Mesozoic THS metasediments with southward verging folds, having Permo-Triassic Kalhel limestone in its core. This can be correlated with similar lithologies of NE-verging Tandi synform in the Chenab valley due to a huge box fold, possibly developed over a ramp in the Main Himalayan Thrust (MHT). These two important opposite verging F2 folds appear to be superposed by large-scale antiformal F3 folds to produce the geometry of a box fold (Hadsar-Chobia box fold - Singh, 2012) during progressive SW translation of this nappe.

This nappe cuts through huge pile of the HHC metamorphics of Zanskar due to top-to-the-SW-downward movement of the THS along the Chenab Shear Zone (CSZ). Since the main HHC belt is not exposed in frontal parts, it is likely to be cut off by the CSZ and splay of the Main Central Thrust (MCT) in the basal parts. An intensely mylonitized 'Outer Granite Band'/Panjal mylonite beneath the low grade THS metamorphics at the base of the Chamba Nappe, thus, represents the subthrust extension of the Kulu-Bajura Nappe of Himachal or the Munsiari Group mylonite of Garhwal (Lahoti *et al*., 2016).

Progressive deformation of the Chamba Nappe since development of the first phase (D1) SW-vergent tectonics resulted in NE-plunging down-the-dip structural and mineral lineations (L1) on equally-prominent foliation (S1) across all the lithotectonic units during ductile shearing and translation of the Chamba Nappe. Subsequent deformation phases second (D2) and third deformations (D3) - produced regional superposed folds and associated axial planar foliations, and appear to be part of the same deformation when the nappe was folded on large-scale due to resistance caused by the foreland in the south.

Himalayan Metamorphic Belt (HMB): Folded HMB is made up of the Tso Morari Crystallines (TMC) in the north, the Higher Himalayan Crystalline (HHC) belt in the middle and the Lesser Himalayan Crystalline (LHC) belt in the south. An extensional Zanskar Shear Zone (ZSZ) or the South Tibetan Detachment System (STDS) separates this belt from the THS. Along its southern margin, this belt is regionally thrust southwards over the LH sedimentary belt along the MCT (Jain, 2015).

(a) Tso Morari Crystallines (TMC): Three different types of amphibole characterize the UHP metamafic rocks of the TMC complex: Na-rich (glaucophane), Na-Ca-rich (barroisite, taramite, winchite), and Carich (tremolite, magnesio-hornblende, pargasite) (Singh *et al*., 2013). The Na-amphibole is present as a core of zoned amphibole with Na-Ca-rich rim; Na-Ca-amphibole is present as inclusion in garnets and matrix, and Ca-amphibole is generally found in matrix. The Na-Ca-amphibole is observed in two different stages of metamorphism. The first is pre-UHP, and the second is post-garnet-omphacite assemblage though with a significant compositional differences. The P-T estimations of formation of these two sets of Na-Ca-amphiboles corroborate their textural associations. Ca-rich amphiboles are generally present in matrix either as symplectite with plagioclase or as a pseudomorph after garn*et al*ong with other secondary minerals like chlorite and biotite. The pre-UHP (or prograde P-T path) and post-UHP stages (or the retrograde P-T path) of Tso Morari eclogite are defined by characteristic amphibole compositions, viz. Na/Na-Ca-amphibole Na-Ca-amphibole and Ca-amphibole and thus indicate their utility in inferring crustal evolution of this UHP terrain.

Further research on UHP metamorphosed TMC by dating outermost ~1.5 micron rims of zircons by SIMS yielded a mean age of 44.9±0.7 Ma with

positive HREE profiles implying the period of zircon growth in the TMC at c. 45 Ma to be retrograde at ~550° to 680°C (Leech *et al*., 2014).

(b) Higher Himalayan Crystalline (HHC) Belt: The Jeori-Wangtu Gneissic Complex (WGC), initially considered as an intrusive into the Rampur Group, was later interpreted as a Proterozoic basement complex (Bhargava *et al*., 2011). Sericite schist having anomalous gradational contact with underlying amphibolite facies complex is explained by considering it as a metamorphosed paleosol developed over the gneiss. This interpretation led to a Paleoproterozoic age of metamorphism of the WGC.

The WGC of the Lesser Himalayan Crystalline sequence experienced superposed folding and doming prior to its exhumation along the Sutlej valley (Sen *et al*., 2012). It forms the basement of the Lesser Himalaya and is bounded by the Vaikrita Thrust (VT) to the northeast and Munsiari Thrust (MT) to the southwest. The regional structure consists of upright large-scale early NW-SE trending folds (D1). The mesoscopic fabric is related to axial plane foliation of the D1 folds and, to a lesser extent, late D2 folds. The axis of maximum compression for D1 and D2 folds are mutually orthogonal. The D1 folds have formed simultaneously with the major Himalayan thrusts, whereas the D2 folds have developed during later deformation. The magnetic lineation in hanging wall of the VT is sub-horizontal indicating stretching along the strike of the thrust. In the interior parts of the WGC, the magnetic fabric is of two types: (i) magnetic lineation demarcates intersection of mesoscopic and magnetic foliation indicating superposed deformation, and (ii) scattered distribution of magnetic lineations due to D2 folding on initially curved and non-cylindrical D1 surface. ^{40}Ar–^{39}Ar dating of biotite from one site in the core of WGC gives an age of 9.3±0.3 Ma (2σ), which is interpreted as the age of doming. It is suggested that effects of superposed folding and ductile deformation of the Himalayan basement rocks have to be taken into account before cross-section balancing or any estimation of crustal shortening is attempted (Sen *et al*., 2012).

On the same WGC, Sen *et al*. (2013) performed magnetomineralogical, petrographic and whole-rock geochemical studies to understand tectonic setting of northern Indian continental margin during the Paleoproterozoic. Although the WGC is dominantly composed of S-type/two-mica granitoids having low magnetic susceptibility (<500 x 10–6 SI units), part of the complex consists of hornblende-magnetite and biotite-magnetite-bearing I-type granitoids with susceptibility greater than 500 x 10–6 SI units. Comparison of magnetic susceptibility with major element concentration reveals that high susceptibility granites are enriched in ferromagnesian and low in silica contents. Tectonic discrimination based on trace element concentration shows that both I- and S-type granitoids of the WGC contain concentration of Y, Nb and Rb, consistent with a collisional/volcanic arc set up, thereby indicating that the North Indian continental margin had an active collisional set up during the Paleoproterozoic (Sen *et al*., 2013).

Mafic and pelitic xenoliths record pre-Himalayan regional metamorphism within early Paleozoic Kinnaur Kailash Granite (KKG) in the Baspa valley, Himachal Pradesh at P-T conditions of amphibolite to granulite facies (Thakur and Patel, 2012; Thakur, 2014). Key evidence of granulite metamorphism is a xenolith of two-pyroxene mafic granulite in which orthopyroxene occurs both as discrete grains and microscopic needles, exsolved parallel to the prismatic cleavage of clinopyroxene host. This xenolith records an average peak metamorphic temperature of 840ºC. Garnetiferous mafic xenoliths display garnet coronae around plagioclase and clinopyroxene, and sphene around ilmenite (Thakur, 2014). These coronae developed by near-isobaric cooling after peak metamorphism at 730ºC and 8 kb. The retrogression path traced by these mafic xenoliths can be constrained through various P-T estimates with temperatures ranging between 536 and 662ºC and pressures from 4.5 to 6.7 kb for formation of corona textures. P-T calculation of garnet-forming reaction rim around clinopyroxene further shows that retrogression had started at ~650ºC and ~7.3 kb, and played a major role in obliterating most of high-grade pre-Himalayan xenoliths from the Himalaya (Thakur, 2014).

In the same early Paleozoic KKG body, pelitic xenoliths have biotite-plagioclase-quartz±garnet±K-feldspar±muscovite assemblage, and record P-T ranges of 7.0-9.0 kb and 500-700ºC, indicating lower to middle amphibolite facies metamorphism (Thakur

and Patel, 2012). In pelitic xenoliths quartz, feldspar and mica commonly show optical evidences of crystallo-plastic deformation indicating that these rocks were sheared before being engulfed as xenoliths in the KKG, implying that present-day shear fabric and metamorphic assemblages in the HHC need not be attributed solely to the Himalayan orogeny.

Along the Sutlej-Baspa valleys, the South Tibetan Detachment (STD) hanging wall is a low-angle normal fault and is characterized by S-type peraluminous Paleozoic (~475 Ma) KKG (Tripathi *et al*., 2012). This granite is later intruded by Cenozoic leucogranite (~18 Ma) in vicinity of the STD zone. Microstructural features and magnetic anisotropy of this granite indicate its intense deformation in vicinity of the STD and preservation of emplacement-related fabric in interior parts. It is inferred that close to the STD zone, fabrics of both the KKG and the leucogranite are tectonic and modified by the Cenozoic (~20 Ma) right-lateral slip and extensional tectonics. Magnetic fabric in interior parts of the KKG is related to its emplacement indicating that original fabric was preserved. U-Pb zircon geochronology of two samples of the KKG yields 477.6±3.4 and 472±4 Ma as the crystallization age. The leucogranite gives an 18.5±0.6 Ma crystallization age (Tripathi *et al*., 2012). It is inferred that deformation of external rim of the KKG and crystallization of leucogranite are synchronously triggered by ductile deformation along the STD.

In the central parts of Uttarakhand Himalaya, more than 20 km thick homoclinally NE-dipping HHC Belt is thrust over the Lesser Himalaya Sedimentary Belt along the Main Central Thrust (MCT), and is almost continuously exposed between Helang and Malari along the Alaknanda and Dhauli Ganga valleys (Shreshtha *et al*., 2015); these have been described stop-wise in much greater details by Jain *et al*. (2015). The upper contact of this belt with the Martoli Formation of the THS is demarcated by the STDS. Thakur *et al*. (2015) recognized the MCT zone within the LH Crystalline Sequence (LHCS), which has gradual contact with the overlying HHC sequence. Using petrographic criteria in pelitic rocks they placed the contact on the basis of (i) first appearance of microscopic kyanite needles, (ii) randomly-oriented inclusion pattern in non-rotational garnet porphyroblasts in contrast to spiral inclusion trails in porphyroblasts of the MCTZ, and (iii) chemically-homogeneous garnet porphyroblasts as opposed to growth-zoned garnets in MCTZ. Pseudosection modelling and garnet isopleths thermobarometry of pelites yielded peak metamorphic conditions of 6.3-7.5 kb and 550-582°C in the MCTZ, and 8.0-10.0 kb and 610-650°C in basal part of the HHCS. The results indicate continuity in P-T field gradient across the contact between the MCTZ and HHCS as well as an inverted metamorphic sequence from biotite to garnet zones in the former.

This whole belt between Helang and Malari is ubiquitously marked by small-scale asymmetrical structures, e.g. S-C and S-C' foliation, porphyroclasts and porphyroblasts, mineral fishes, intrafolial folds, duplex structures, ductile-brittle shear zones, and asymmetric shear boudins (Shreshtha *et al*., 2015). Ductile to brittle-ductile shear sense, determined from these structures across the whole belt, the MCT and the STDS, reveals two phases of shear deformation: (a) an older top-to-SW upwards phase throughout the HHC, having an overall thrust geometry (DS1), and (b) a younger superposed top-to-NE downwards phase with normal fault sense from the middle to upper parts (DS2). These shear senses provide invaluable constraints on various tectonic models currently in use for the evolution of the Himalayan metamorphics.

Wiedenbeck *et al*. (2014) performed single zircon Pb/Pb age determinations on five samples from the Garhwal Himalaya, where extensive Paleoproterozoic volcanic and plutonic activity took place. Interbedded acid volcanic band indicated a depositional age of ~1.86 Ga for the upper part of the Berinag Group. Three deformed granitoids from the lowermost Munsiari Thrust sheet yielded $^{207}Pb/^{206}Pb$ ages between 1.85 and 1.74 Ga, which reflected the crystallization age of these rocks. In contrast, sample from a paragneiss located towards the base of the Vaikrita Thrust sheet, yielded a minimum age of <l.0 Ga suggesting that Vaikrita represents the second distinct stratigraphic unit of the Higher Himalaya.

In the uppermost parts of this belt along the Dhauli Ganga valley in Garhwal, Jain *et al*. (2013) recorded widespread *in situ* partial melting of sillimanite+K-feldspar gneiss which produced migmatite and resultant melt accumulation near the STDS during various deformation events. The oldest migmatite phase, designated as the Me1, parallels the

main foliation Sm as concordant stromatite layers and leucogranite bands. Younger melt phases Me2, Me3 and Me5 are recorded along small-scale ductile thrusts, extensional fabric and structureless patches, respectively. It is only the Me4 melt phase that is evidenced by large-scale melt migration along cross-cutting irregular veins. These were possible conduits for migration and accumulation of melt into larger leucogranite bodies like the Malari leucogranite at ~19.0±0.5 Ma.

Bulk rock geochemical analyses of the Greater Himalayan Sequence (GHS) along these valleys in Garhwal show chemical index alteration (CIA) values of 57-93 with an average of 67, average (La/Yb)N=18.6, average (La/Sm)N=3.7, Cr/Th between 0.2 and 214.5, and Th/Sc range between 0.2 and 10.3 (Spencer *et al*., 2011). Various geochemical tectonic indicators reveal signatures akin to an active continental margin with proximal and primarily silicic source region. Occurrence of three-phase halite-bearing primary fluid inclusions in quartz grains from metasediments, moderately high temperature bi-aqueous inclusions, and carbonic-aqueous inclusions estimate maximum salinity at ~33 wt.% NaCl indicating their provenance from a magmatic terrain. Potential source regions of the GHS are the East African Orogeny, the East Antarctic Orogeny and/or the Bhimpedian Orogeny of Northern India (Spencer *et al*., 2011).

In the eastern parts of the HHC along the Kaliganga Valley at the India-Nepal border, Rao *et al*. (2014) observed granite gneiss, biotite-garnet gneiss, migmatite, quartzite, coarse grained augen gneiss, and biotite-kyanite/sillimanite schist. Peak metamorphism M2 was attained during the D2 deformation, and is represented by main S2 foliation with preferred oriented micas, staurolite and kyanite/sillimanite; the S1 foliation is preserved in poikiloblastic garnet as discontinuous S_i (Rao *et al*., 2014). P-T estimates of 4.5 kb and 475°C are inferred in the lower parts of the section, while 11 kb and 850°C for garnet-kyanite schist in upper structural levels corresponding to tectonic burial depths of 15 to 37 km, and geothermal gradient variation of 32°C/km to 22°C/km in the region. The observed maximum P-T differences of 6.5 kb and 375°C up-section infer dP/dT of ~17 bars/^{o}C, thereby suggesting possible isothermal decompression uplift path.

In the eastern parts of the Himalayan orogen (Darjeeling-Sikkim Himalaya) detailed structural, metamorphic and geochronological investigations have provided insight into its crustal shortening, P-T conditions and timing of metamorphism. In the Darjeeling-Sikkim Himalayan fold thrust belt (FTB), a minimum shortening of ~450 km (~81%) is accommodated south of the STDS in a folded thrust system (Bhattacharyya *et al*., 2015a). From north to south these are the Main Central thrust (MCT), the Pelling thrust (PT), the Lesser Himalayan duplex, the Ramgarh thrust (RT), the Main Boundary thrust (MBT) and the Main Frontal thrust (MFT). The average long-term shortening rate is estimated at ~20 mm/yr (Bhattacharyya *et al*., 2015a). The initial width of the Lesser Himalayan (LH) basin controlled the geometry and total number of LH imbricates and horses along the FTB, thereby controlling the minimum shortening estimates from the orogenic transects (Bhattacharyya and Ahmed, 2016).

The Pelling thrust (PT) accommodated translation ~100km along a thin mylonite zone (~2-24 m) by different mechanisms of strain softening along different segments of its transport direction (Bhattacharyya and Mitra, 2014). The geometry of tapered crystalline orogenic wedge caused variation of overburden (~12-21 km) along the PT mylonite zone that resulted in different deformation conditions along the studied segments. The PT also forms linear, discontinuous, klippen within the Teesta window that record local, orogen-parallel strong constrictional strain (k~6; Bhattacharyya *et al*., 2015b). This is manifested by N-S trending L tectonite that lie in spatial association with LS and SL tectonite (Bhattacharyya *et al*., 2015). These klippe are folded along gently plunging, transport-parallel, N-S trending synform with the strongest L fabric developed along the hinge zones. We integrate structural geometry and strain analyses to propose the possible existence of a lateral ramp beneath the PT sheet to explain the local, orogen-parallel constrictional strain and transport-parallel fold in this region (Bhattacharyya *et al*., 2015b).

In the Ramgarh thrust sheet of the Darjeeling-Sikkim Himalaya, Banerjee *et al*. (2015) observed metre-to centimetre-scale late-stage folds on foliation in phyllite with near-recumbent fold geometry, which developed with a specific spatial distribution, particularly in places where the foliation is steeply

dipping. The recumbent fold structures appear to have been formed in response to overburden-induced vertical compressive deformation on steeply-dipping foliation due to gravity and overburden, especially in the subvertical southern limb of the antiformal structure of the Lesser Himalayan Duplex.

Bulk of petrological work in this segment of the Himalaya focussed on metapelites, gneissic rocks and eclogitic mafic rocks, while non-eclogitic mafic lenses in metapelites, occurring both in the Lesser- and Higher Himalayan domains, were hardly looked into. Such mafic lenses have identical sub-alkaline tholeiitic basalt affinity and were metamorphosed at 9-12 kb and 800ºC (Faak *et al*., 2012). Peak P-T conditions of these metabasites are independent of geographic or tectonic location of samples and they differ in their mineralogy and P-T conditions from regionally-metamorphosed metapelites (i.e., metapelites not at immediate contact of metabasites). The retrograde P-T path of the LH and HH metabasites are different: the HH samples underwent steep decompression, whereas the LH samples followed a relatively gentle exhumation path. The metabasites along with the immediately adjoining metapelites are interpreted to be slivers emplaced within the regionally metamorphosed metapelites indicating thermal perturbation at the base of the crust of average thickness.

Geo- and thermochronological methods to study the deformation and cooling history of footwall rocks of granulites and local granulitized eclogites along the STDS in northern Sikkim demonstrate that it was active between 23.6 and ~13 Ma, and that footwall rocks cooled rapidly from ~700 to ~120°C between ~15 and 13 Ma (Kellett *et al*., 2013). While active, the STDS exhumed rocks from mid-crustal depths, but an additional heat source such as strain heating, advected melt and/or crustal thinning is required to explain the observed isothermal decompression. Cessation of movement on this system produced rapid cooling of the footwall as the isotherms relaxed.

Extending an earlier petrological investigation on Lesser Himalayan metapelites of the Sikkim Himalaya (Dasgupta *et al*., 2009, Amer. Jour. Sci., v.309, p. 43-84), Gaidies *et al*., (2015) modelled garnet crystallization in garnet- and staurolite zone metapelites utilizing Gibbs Energy Minimization, multicomponent diffusion theory and a nucleation and growth algorithm (Theria, G.). The unique feature of this study is that crystallization of garnet is modelled at incremental steps with changing bulk composition as new garnet nucleates. The mineral assemblages and garnet zoning are consistent with tight clockwise P-T paths that are characterized by prograde gradients of ~30ºC/kb for garnet zone rocks and ~20ºC/kb for staurolite zone rocks. According to the calculations, garnet stopped growing at peak pressures, and protracted heating after peak pressure was insignificant. The results are consistent with a model of tectonic inversion of a coherent Barrovian package. From excellent preservation of growth zoning in garnets from the Lesser Himalayan metapelites, we argue for very short timescales of metamorphism.

Detailed petrography, identification of mineral reactions, petrogenetic grids, kinetically constrained thermobarometry and pseudosection calculations of the Sikkim HHC led Sorcar *et al*. (2014) to conclude peak P-T conditions of 9-12 kb and 750-800ºC in migmatites, followed by steep isothermal decompression to 3-5 kb, and then isobaric cooling to ~600ºC. Decompression is inferred to be triggered by production of ~20% of melt in the package. Geospeedometry indicates necessity of a two-stage cooling history in order to satisfy the compositional zoning in garnets. Both of these stages are rapid (~100ºC/Ma between 800-600ºC, followed by several 10'sºC/Ma between 600-500ºC), but we recorded contrasting cooling histories in apparently homogeneous package of the HHC. Rocks lying close to the STDS cooled more rapidly than those occurring to the south. The boundary between the two domains lies close to the discontinuity in age recorded by another study from our group (see below, Rubatto *et al*., 2013).

Rubatto *et al*. (2013) carried out extensive trace elemental and geochronological studies on the HHC of Sikkim, using SHRIMP and LAICPMS on zircon and monazite to ascertain conditions of formation. Systematic variations in compositions of the dated mineral zones (HREE content and negative EU anomaly) are related to variations in garnet and K-feldspar abundances respectively, and thus to metamorphic reactions and P-T stages. Melting occurred over ~15 Ma (31-17 Ma) in the Higher Himalaya, but a given block traversed the melting

interval in 5-7 Ma. In the Sikkim HHC, the higher structural levels reached melting conditions later (~26-23 Ma) than the lower structural levels (~31-27 Ma). Interestingly, the two blocks evolved through different cooling patterns (see Sorcar *et al*., 2014 above). Therefore, from both geospeedometry and geochronology, we identify a tectonic discontinuity in the apparently homogeneous HHC in Sikkim Himalaya.

Anczkiewicz *et al*. (2014) used Lu-Hf systematics in garnets from the Lesser and Higher Himalayan metapelites as well as Lu zoning patterns in garnets to show that there is a systematic increase in age of crystallization of garnet towards the MCT (10.6±0.2 Ma in garnet zone and 14.6±0.1 Ma in sillimanite zone, and 16.8±0.1 Ma in muscovite melting zone below the MCT). Lu zoning patterns conform to Mn growth zoning patterns in rocks below ~biotite melting interval, and therefore the obtained ages correspond to crystallization age of garnet. The total span of Barrovian metamorphism has been estimated as ~6 Ma, while individual garnets grew over a time interval of ~0.5 Ma. The Lu-Hf ages in biotite melting zone (Higher Himalaya) correspond to the time of partial melting and are distinctly older (22.6-28 Ma). The age patterns provide precise time constraints on the continental collision models, the protracted older melting history of the Higher Himalayas (see Rubatto *et al*., 2013, as discussed above) and progressively younger age of garnet crystallization in the Lesser Himalaya as one moves away from the MCT.

The MCT in the Sikkim Himalaya is recognized, as in many other parts of the eastern Himalaya, as a wide zone of distributed ductile and simple shear deformation. Mottram *et al*. (2014) suggest an alternative method of discriminating the contact, by using the isotopic signature of blocks across the shear zone as a marker of the position of the MCT. They suggest that the GHS and the LHS represent terranes with distinct isotopic signatures that have been brought together by movement along the MCT. The GHS is characterized by detrital zircon age peaks around 800-1000 Ma, 1500-1700 Ma and 2300-2500 Ma, and by an $\varepsilon Nd(0)$ signature of –18.3 to –12.1. This rock package was intruded by granites of Neoproterozoic (c. 800 Ma) and Ediacaran-Cambrian (c. 500-600 Ma) age. In the footwall, the Daling Group of rocks of the LHS comprises a Paleoproterozoic rock package with prominent Archean and Paleoproterozoic detrital zircon populations and an $\varepsilon Nd(0)$ signature of –27.7 to –23.4. These isotopic signatures show interfingering across the ductile shear domain, which the authors interpret as evidence of "out-of-sequence thrusting in the course of ongoing MCT-related deformation".

De Sarkar *et al*. (2013a) documented well-developed arc-perpendicular normal faults and arc-parallel sinistral strike-slip faults as evidences of active Quaternary E-W arc-parallel extensional features in the Lesser and Higher Himalaya in western part of Arunachal. Occurrences of these arc-parallel extensional structures are interpreted in terms of oblique convergence and radial expansion models due to stress partitioning. The estimated amount of arc-parallel extension is ~110 km for the NE Himalayan segment.

In the Siyom Valley of Arunachal Himalaya, Nandini and Thakur (2011) delineated classical Barrovian inverted metamorphism in the LH Crystalline Sequence on the western limb of the Siang antiform from biotite zone through garnet-, staurolite-, kyanite-, sillimanite- to sillimanite-K-feldspar zone with granulite-facies pelitic assemblages of garnet+cordierite with increasing grade at higher structural level. Three phases of F_1, F_2 and F_3 folding and two generations of S_1 and S_2 planar structures are recognized. Metamorphic isograds and boundary thrusts are co-folded around the Siang antiform by F_3 deformation. Garnet shows prograde growth zoning in lower grade rocks and retrograde diffusion zoning in higher grade rocks. Pelites of the sillimanite-K-feldspar zone show textural evidence of decompression such as cordierite corona around kyanite. Breakdown reactions of muscovite and biotite in this zone are attributed to decompression. Geothermobarometric calculations show gradual increase of temperature to sillimanite-K-feldspar zone, whereas pressure increases sharply from garnet zone to staurolite zone and remains nearly constant thereafter (Nandini and Thakur, 2011). Peak metamorphism reached P-T conditions of ~10 kb and >750°C in sillimanite-K-feldspar zone. P-T estimates, decompression reactions and pseudosection topologies suggest a clockwise path with steep decompression for the evolution of sillimanite-K-feldspar zone in Siyom Valley.

(c) Lesser Himalayan metamorphic belt: Extensive mapping of the Jutogh Group metasediments of the Jutogh Thrust Sheet (JTS) revealed that these occur in the Simla Klippe and the Chaur Mountain Belt (Bhargava and Srikantia, 2014); the latter extending up to the Pabbar Valley and beyond to the Satluj Valley. The Jutogh group is divisible into 11 formations; out of which lowermost Panjerli Formation is mainly carbonaceous schist with limestone and quartzite bands. The overlying Manal, Khirki, Kanda, Badrol and Chirgaon formations are mainly quartzitic sequences with local schist bands, while the Bhotli, Taradevi, Naura, Rohru and Jaknoti chiefly comprise schist, selectively carbonaceous, with limestone/marble, quartzite and gneiss bands. The Chaur and Kainchwa Granitoid complexes occur within the Naura Formation. The Jutogh Thrust tectonically overlaps the Kulu Thrust Sheet south of Baragaon and rests over the Jaunsar Group. The Kulu Thrust Sheet reappears near Kharsali. The Jutogh Group is succeeded by the Vaikrita Group along a thrust.

The metamorphism in the Jutogh and Vaikrita rocks varies from low grade to medium-high grade with development of greenschist facies in the Panjerli and Manal formations (Bhargava and Srikantia, 2014). The Bhotli and Taradevi formations, occurring at the sole of the JTS due to recumbency, also display greenschist facies. Greenschist-amphibolite transitional facies is reflected in the Bhotli, Khirki, parts of the Taradevi and Badrol formations. Typical amphibolite facies is observed in parts of the Taradevi, Kanda, Naura, Rohru, Chirgaon, Jaknoti and Sundru formations. Amphibolite-Granulite Transition Facies is locally present in the Naura and Sundru formations and the associated coarse granitoid gneiss. Xenoliths of the Naura schist are present in the non-foliated granite and display hornfelsic textures. The rocks of the Vaikrita Group are quite similar to those of the Jutogh Group and may represent a deeper digitation of the JTS.

The Jutogh rocks, bounded by the synformally folded Jutogh Thrust, represent the most southerly transgressed thrust sheet in the Western Himalaya. Out of the five generation of folds first two folds (reclined/recumbent) are oriented in E-W direction. These being athwart the structural trend in the Western Himalaya are possibly of pre-Himalayan age. The third (reclined/recumbent, syn-transport) and fourth of regional dimension (mostly upright to overturned) folds have a NW-SE trend; the latter have determined the trend of the structural belts and even that of the orographic axes. The fifth generation folds are NE-SW trending cross- folds. High-angled faults affecting all the folds constitute the last tectonic event in the area (Bhargava and Srikantia, 2014).

The Naura Formation, in its upper part in the vicinity of the Chaur Granitic Complex shows development of large-sized garnet and staurolite crystals. Garnets up to 10 cm in diameter are confined to mica schist bands within the gneiss. These garnets cut across the main foliation and represent syn- to post-kinematic growth with respect to the main foliation.

Two garnet crystals (JU1, JU2), collected from Deola (30°48'30.9":77°25'16.20"), each ~3 cm in size, were dated by the Sm-Nd on TIMS (Bhargava *et al.*, 2015). These have inclusions of quartz, plagioclase, ilmenite, apatite, biotite, chlorite, micro-zircon, and, importantly, JU2 garnet also contains inclusions of staurolite. Garnet crystal JU1 yielded a Sm-Nd isochron regression age of 485±19 Ma (n=8; MSWD=6.6; εNd=–6.1), while its rim part alone gave an age of 473±14 Ma. Crystal JU2 gave an age of 480±11 Ma (n=5; MSWD=4.0; εNd=–5.9); its rim part alone yielded an age of 477.9±6.2 Ma. Combining

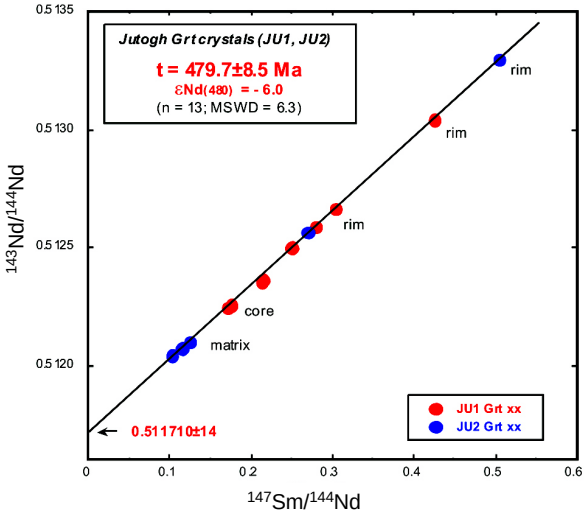

Fig. 1: Sm-Nd isochron plot for 13 fractions of two cm-sized single garnet crystals from the Naura Formation, Jutogh Group. Mean regression age of 479.7±8.5 Ma indicates time of garnet crystallization during an Early Ordovician tectonometamorphic event

all analyses in one regression calculation, resulting age is 479.7±8.5 Ma (n=13; MSWD=6.3; εNd=–6.0) (Fig. 1). This "mean age" is interpreted as the time of garnet crystallization. The results imply that garnets crystallized within one single coherent metamorphic event in the Early Ordovician (480±10 Ma) and there is no indication that the more inclusion-rich core parts of garnets are significantly older than their idiomorphic rims (Bhargava *et al*., 2015).

Reorientation of linear structures and their low scatter in direction of bulk shear along crustal-scale MCT in Munsiari-Milam area of eastern Kumaon could be related to strong ductile shear deformation along this thrust (Verma and Bhattacharya, 2011).

Further south, base of the Almora Crystallines developed dark-coloured folded pseudotachylite veins of irregular thickness in mylonite along the South Almora Thrust (SAT) zone in Kumaon Lesser Himalaya (Agarwal *et al*., 2011). Intense deformation and frictional heating was responsible for producing small melt in thin sharp veins during thrust sheet movement. Deformation near the SAT has a consistent top-to-south shear sense.

The AMS study of the Almora Crystalline Zone (ACZ) reveals that magnetic fabric is carried by secondary paramagnetic minerals. Near the SAT in the sedimentary beds, metamorphic and magnetic foliations have similar northern dips (Agarwal *et al*., 2016). The situation near the NAT is complex; here general trend of these fabrics is southward-dipping, corresponding k3 plunges northwards with some k3 demonstrating a southward plunge. However, near the NAT, both top-to-south and top-to-north shear senses are recorded. It is thus proposed that the Lesser Himalayan NAT was back-thrust after the emplacement of the ACZ.

Neotectonics in active Himalayan terrain in the Kali River System, Kumaon has been deciphered from drainage incision by identifying tilting of Quaternary blocks and is of great utility in areas where active faults are concealed or poorly exposed (Agarwal and Sharma, 2011). Drainage pattern of the Ladhiya and Lohawati basin is structurally-controlled and neotectonically active. Landslides, river terraces, vertical down-cutting of the rivers, their deep gorges, triangular facets (flatirons) and tilting of beds record such an activity. In some basins, morphometric parameters suggest a possibility of flash floods and high discharges (Agarwal *et al*., 2012).

Use of satellite imagery and morphometric analysis of SukhRao basin in a NW-SE trending synclinal trough south of Paonta Sahib in Sirmur district of Himachal Pradesh indicate that tectonic blocks have moved, tilted and skewed sinistrally forcing the SE flowing Giri, Bata and SukhRao streams to take sharp southward trend along the segments of the Yamuna tear (Srivastava, *et al*., 2012). The NE-SW trending syngenetic transverse faults have induced stream piracy through fast erosion.

Lesser Himalayan Sedimentary Belt

McKenzie *et al*. (2015) discussed the evolution of the north Indian continental margin in the light of new geochronologic, biostratigraphic and geochemical data generated on several Proterozoic sedimentary succession of the Indian subcontinent. A regional ~500 Myr unconformity has been postulated between Late Paleoproterozoic and late Mesoproterozoic strata across northern India.

A detailed review of the carbon and sulfur isotopic analyses of carbonates of Ediacaran strata in the Lesser Himalaya (Banerjee, 2013) provided significant information about the oxidative state of the marine realm prevailing during the late Proterozoic times. This study helped in interpreting the intimate and causative association of pyrite, phosphorite and black shale

Trace fossils *Psammichnites gigas, Monomorphicnus, Palaeophycus* isp. and ?*Hormsiroidia* are discovered at 98m above the base of the Arenaceous Member (Tal Group) of the Early Cambrian age in the Mussoorie Syncline (Singh, 2011). The level occurs much below the *Drepanuroides* Zone of early Tsanglangpuion Stage. The ichnofossil assemblage with respect to trilobite level indicate upper Tommotian-Lower Atdabanian age (=Zone III of Crimes, 1987, Geol. Mag., v. 124, p.97-119).

Archaeonassa was recorded from the lower part of Siltstone Member of the Sankholi Formation (Tal Group) at Ganog locality in the Nigali Dhar Syncline (Singh *et al*., 2015). This is the first record of this ichnotaxa from the Cambrian succession of the Himalaya. The ichnofossil is attributed to locomotion of mollusc-like animal close to sediment

water interface, pointing to shallow marine environment of deposition.

Shaanxilithes ningoiangesis, an enigmatic fossil, variously regarded as algae, trace fossil and also as body fossil reported from the Earthy Dolomite Member (Krol Group) and Earthy Siltstone Member of the Shaliyan Formation (Tal Group) from the Nigali Dhar Syncline, has been considered as organic-walled tubular body fossil of unknown taxonomic affinity (Tarhan *et al*., 2014). This fossil has potential in delineating Precambrian/Cambrian boundary in the Lesser Himalaya. The fossils consist of compressed organic cylindrical structures, characterized by extended, overlapping or fragmented iterated units. Lithologic comparisons and sequence stratigraphic data all suggest a late Ediacaran age for the uppermost Krol Group and basalmost Tal Group. The biogeographical distribution of *S. ningqiangensis*, hitherto confined to the Ediacaran of China and potentially Siberia, to the Precambrian-Cambrian boundary interval of India, enlarges its biostratigraphic utility to the inter-regional and inter-continental scale.

Tiwari *et al*. (2013) have reported nine ichnotaxa, *Dimorphichnus* isp., ?*Diplichnites* isp., *Monomorphichnus* isp., *Nereites* isp., *Palaeopasichnus*isp., *Palaeophycus* isp., *Planolites montanus*,*Planolites* isp., *Skolithos* isp., *Treptichnus* isp. from Early Cambrian Dhaulagiri Formation of the Tal Group, indicating that it was deposited under shallow marine fluctuating energy conditions with turbid water fluxes.

From a new locality of Maldevta-Chhimoli, Mussoorie Syncline *Cruziana* Assemblage Zone III, having an assemblage of *Bergaueria perata*, *Cochlichnus anguineus*, *Glockeria* isp., *Helminthopsis* isp., *Monomorphichnus lineatus*, *Phycodes palmatum*, *Palaeophycus striatus*, *Planolites beverleyensis*, *P. montanus*, *Tretichnus* cf. *Pedum* (Singh *et al*., 2014). This assemblage occurring between the *Drepanuroides* and *Paleoolenus* trilobite zones is assigned Cambrian Series 2 in a shallow marine setting.

Magmatism in the Himalaya

Proterozoic granitoids from the Lesser and Higher Himalayas of western Arunachal Himalaya are massive and foliated, porphyritic, hypidiomorphic and rarely porphyroblastic (Srivastava, 2013). Observed geochemical characters of these granitoids, such as their peraluminous and alkali-calcic/calcic-alkalic nature, different multi-element and rare earth element patterns, together with low Mg# (Mg number) suggest their derivations from lower crustal material rather than a mantle source. It is difficult to explain variations in granitoids by partial melting alone. Different other processes like migration of melts, magma mixing, assimilation and fractional crystallization also played important role in the genesis of these granitoids. These melts were likely generated at low temperature (730-760^{o}C) and low pressure (2-5 GPa), and are emplaced within the syn-collisional tectonic setting, while a few granitoid samples also indicate their volcanic-arc nature (Srivastava, 2013).

Evolution of Himalayan Foreland

Sequence stratigraphy of the Subathu Formation and a part the Dagshai Formation was erected in the Himalayan Foreland Basin of Shimla Hills, where the former (Late Thanetian-Early Priabonian) constitutes a 2nd order depositional sequence with a subaerial unconformity at the base and a tidally-influenced transitional sequence at the top (Bhatia *et al*., 2014). Three 3rd order T-R successions - A, B and C are recognized. Succession A (late Thanetian-late early Cuisian) includes seven facies associations (FA) and commenced with transgression (TST), followed by MFS and a condensed section (P4, SBZ 4-9), carbonate-siliciclastic coarsening upward sequence (HST), tectonically-driven deposits, formation of back barrier lagoon with tidal inlet inhabited by sharks, ray fish; poor circulation in the lagoon, caused mortality of vertebrate fauna and Early stage base level rise. Succession B (Middle-Upper Cuisian, SBZ 11-12) includes seven facies: Minor flooding surfaces, Coarsening upward succession, Tidal flat, Subtidal setting, Muddy tempestites in inner shelf, Rise in sea level indicated by several benthic foraminifera and crabs, and Amalgamated sequence of proximal tempestites of shoreface in inner shelf setting. Succession C (Early Lutetian-Early Priabonian) constitutes four facies beginning with flooding marked by *Assilina spira abrardi* zone, succeeded by Biotic condensation passing into the Passage Bed (FSST) displaying textural inversion in delta influenced setting, and coastal sand (White Quartzarenite). Conformably overlying basal part of the Dagshai Formation

comprises three tidally-influenced parasequences (LST) separated by two calcrete levels.

Singh *et al*. (2013) investigated relationships between Late Miocene C4 grasslands and CO2 levels in the Mio-Pleistocene Siwalik paleosols in Ramnagar sub-basin along with the Oligocene Dagshai paleosols, exposed in the Subathu sub-basin by conducting stable carbon isotope analyses on 141 pedogenic carbonates. These results show dominance of C3 vegetation pre-7 Ma and dominance of C4 vegetation post-5 Ma. Percentage abundance of C4 vegetation was less than 20% pre-7 Ma but increased to more than 40% post-5 Ma, reaching up to 100% in the youngest analyzed sediments. There is exclusive dominance of C3 vegetation during the Oligocene. These results conform the changing vegetation patterns, documented in other parts of the Himalaya. Global expansion of C4 grasslands largely during Late Miocene have been linked to declining atmospheric CO2 level, large-scale fires, intensification of monsoon, seasonality and aridity, which are not very convincing due to significant shortcomings associated with them. They suggested that initial lowering of CO2 below 450 ppmV created an environment for beginning of C4 vegetation, but persistence of this threshold value for a considerable time during Late Miocene appears to be the probable cause of global expansion of C4 grasslands during this period irrespective of their time of first appearance. It has been deduced through correlation of the Himalayan tectonic events with atmospheric CO2 levels and paleovegetational changes since Upper Miocene times that it was indeed the Late Miocene continuous, intense tectonic instability of the Himalaya that significantly decreased atmospheric CO2 levels and perhaps played a key role in changing nature of photosynthetic pathways.

Srivastava *et al*. (2013) reported paleopedological features of fossil soils that formed during the earliest phase of continental sedimentation of the Dagshai Formation in the NW Himalayan foreland. This fluvial sequence (31.6±3.9 to 30.3±3.9 Ma) along the Koshaliya River contains four pedofacies A-D of ferruginous paleosol sequences within overbank sediments. Pedofacies A consists of 3-4 well-developed ferruginous paleosols overlain by gray sandstone beds. Pedofacies B-D are marked by a progressive decrease in pedogenesis. These paleosols occur as 0.5 m to 1.5 m thick horizons that are marked by extensive development of rhizoliths, pedogenic carbonate and iron-rich clay pedofeatures that correspond to modern Entisols, Inceptisols, Alfisols and Vertisols. It is inferred that these paleosols were formed at ~18°N paleolatitude in the Dagshai sub-basin, based on early Oligocene paleogeographic position of northward-drifting Indian Plate. Micromorphology, geochemical analyses, weathering indices, and stable isotope composition of paleosols indicate tropical climate (paleoprecipitation of 947-1256 mm and paleotemperature of ~25°C) with an initial phase of monsoonal conditions during pedogenesis. These paleoclimatic conditions favored C3 paleovegetation immediately after transition from greenhouse to icehouse conditions.

Pandey *et al*. (2014) investigated the Quaternary-Holocene landforms of the Dun Valley in frontal NW Sub-Himalayan Belt, where they observed front parallel longitudinal valleys, occupying the synformal troughs. The perennial glacial-fed Ganga and Yamuna rivers experienced first major gradient loss along this valley floor and produced characteristic landforms and deposits by gradational streams processes that are often controlled by climate fluctuation. In the Dun valley, barring an isolated patch of ~26 and 20 ka-old terrace, no strath terrace older than the Holocene is observed along these rivers. A large stretch of this valley is filled in by piedmont deposits that started aggradation since >40 ka until the beginning of the Holocene and have since been undergoing incision. A similar trend is observed in the upper Ganga valley, where multiple Late Quaternary aggradational terraces are observed. They attempted to understand the role of Late Quaternary-Holocene climate fluctuations and their effect on associated gradational processes from these landforms and associated deposits..

The Middle Siwalik Subgroup of Darjeeling Himalaya along Tista river valley has been repeated by a number of north-dipping thrusts and shows temporal repetition of sedimentary facies associations suggesting oscillation between proximal-, mid- and distal fan setups within a palaeo-alluvial fan depositional environment (Kundu *et al*., 2012). This depositional setup of the Siwalik is probably due to a combination of foreland-ward movement of the Himalayan thrusts, climatic variations and mountain-ward shift of fan-apex due to erosion. These sediments

were derived from Higher and Lesser Himalayan rocks in humid climatic conditions similar to moist humid climate of the present-day Eastern Himalaya.

Recent studies of the Cambrian deposits of the "upper Lesser Himalaya" succession of the "outer" Lesser Himalaya tectonic unit indicated that these are enriched in radiogenic ^{187}Os (Myrow *et al*., 2015). They make up part of a proximal marine facies belt and in contrast age equivalent facies in the Tethys Himalayan succession are more distal in nature. These authors suggested that exhumation and weathering of the upper Lesser Himalaya and related strata caused dramatic changes in the $^{187}Os/^{188}Os$ and $^{87}Sr/^{86}Sr$ Neogene record of seaways starting at ~16 Ma.

Exhumation

In the NW Himalaya, fission-track apatite and zircon data from the Higher Himalayan Crystallines (HHC) along the Kaliganga, Darma and Goriganga valleys in Kumaon exhibit similar age range and exhumation history indicating uplift and exhumation of this belt as a single block, in general (Patel *et al*., 2011). These FT data are consistent with steady-state exhumation since ~2 Ma with erosional effluxes balancing the tectonic influx, while such steady-state exhumation condition was achieved in south of the MCT/MT since 9 to 14 Ma within the Chiplakot Crystalline Belt (CCB). Since young FT ages are concentrated in hanging wall of the MCT/MT and VT, tectonics along these valleys is viewed as the major factor for faster uplift of the HHC; uniformly rapid erosion is linked to long-term uniform precipitation throughout Kumaon Himalaya. On the other hand, older exhumation ages south of the MCT/MT reflect no reactivation of duplex structures through which the CCB was emplaced over the meta-sedimentary rocks of the LHS zone since Miocene time.

Along the Pindari River in Garhwal region, the AFT ages show linear southward younging from 4.2±0.7 to 2.1±0.2 Ma with abrupt jumps across strike of major thrusts, namely the VT, the MT/MCT and the Berinag Thrust (BT) (Singh *et al*., 2012). Break and displacement in age pattern with youngest ages close to thrusts are described due to progressive late thrust movement reflecting the in-sequence style of thrust propagation, uplift and cooling towards south from the VT to BT. Activation of the VT before ~2.5 Ma was followed by activation along the BT in the south, possibly before 0.3 Ma, based on offset and sequential younging of cooling ages (Singh *et al*., 2012).

From the Dalhousie Granite of Dhauladhar Range, apatite (2.9±0.2 to 4.4±1.0 Ma) and zircon FT ages (10.4±1.4 to 21.1±2.2 Ma) suggest slow exhumation during Middle to Late Miocene, followed by acceleration during Plio-Pleistocene (Adlakha *et al*., 2013a). Activity along the Panjal Thrust (PT)/ MCT ceased at ~15 Ma in this region, while tectonic activity started prior to ~10 Ma along the Main Boundary Thrust (MBT). Tilting of topography due to activation of the MBT controls the exhumation pattern of Dalhousie Granite during Middle to Late Miocene (Adlakha *et al*., 2013a).

AFT cooling ages in the Lesser Himalaya are quite older than the HHC and range from 4.7±0.5 and 6.6±0.8 Ma in the Baijnath klippe, 3.7±0.8 to 13.2±2.7 Ma in the Almora klippe, and 6.3±0.8 to 7.2±1.0 Ma in the Ramgarh thrust sheet (Patel *et al*., 2015). Thrusting and back-thrusting within the Almora klippe and Ramgarh thrust sheet reveal post-emplacement kinematics that controlled the exhumation of the Almora klippe.

In the northeast Himalaya of western Arunachal, AFT and ZFT bedrock ages within the rain shadow of the Shillong Plateau demonstrate that spatial gradients in precipitation do not correlate with variations in millennial-scale erosion rates (Adlakha *et al*., 2013b). 3D- thermal-kinematic modelling of thermochronometric data suggests that out-of-sequence fault south of the MCT initiated between 6.5 and 8.5 Ma and local exhumation patterns are controlled by rock uplift of the region, which is dictated by fault kinematics in this rapidly deforming area (Adlakha *et al*., 2013b).

From the same western Arunachal, combined results from Raman thermometry and thermochronological record demonstrate that upper zones of the HHC ~ 20 km north of the MCT cooled below the ~350-400°C at~13 Ma, while middle zone exhumed at ~11 Ma and lower zone close to MCT at ~8 Ma indicating erosional unroofing of the MCT sheet (Mathew *et al*., 2013). Based on AFT and ZFT ages of Adlakha *et al*. (2013b), it is inferred that peak metamorphic temperatures were achieved prior to at least~14 Ma ago between regions south of the MCT zone and upper MBT.

Optically Stimulated Luminescence (OSL) dating technique on quartz (closure temperature ~30-35°C) suggests increased erosion rates over a period of ~21 ka for the period from Late Pleistocene (2.5 mm/yr) to Early Holocene (5.5 mm/yr) for the HHC of western Arunachal Himalaya (De Sarkar *et al*., 2013b).

Adlakha *et al*. (2013c) reviewed exhumation concept and mechanisms with reference to Himalaya.

Paleoseismology and Convergence Rates

Active fault mapping (AFM), trench investigations across the active fault scarps, liquefaction features and archeo-seismology all converge towards understanding the pattern of strain release in the Himalaya and, thus, draw inference towards characterization of the Himalayan earthquake cycle (Fig. 2).

In the Riasi area of the NW Himalaya, Medlicott-Wadia Thrust (MWT, formerly known as Main Boundary Fault) and Himalayan Frontal Thrust (HFT) consume shortening rates between 13.2-27.2 mm/yr since 14-24 ka (Fig. 2; Vassallo *et al*., 2015). Their geological intermediate shortening rates are not in harmony with current rate of 13.6±1 mm/yr convergence deduced from the geodetic survey across the Kashmir Himalaya (Kundu *et al*., 2014), thereby implying an unsteady deformation pattern in this region of the NW Himalaya. The causative Balakot-Bagh Fault of the 2005 Kashmir earthquake extends SE with right-step to the Riasi Thrust, which was previously referred as the MBF by Wadia in Jammu region. Further SE extension of the Riasi Thrust has been mapped with different nomenclature to the 1905 Kangra earthquake meizoseismal region, suggesting linkage between the earthquake and the active fault. There is no historical record of a large magnitude Mw >7 event for the last ~1000 years in eastern segment of Kashmir seismic gap, which may imply ~12 m slip deficit in the region (Thakur and Jayangondaperumal, 2015).

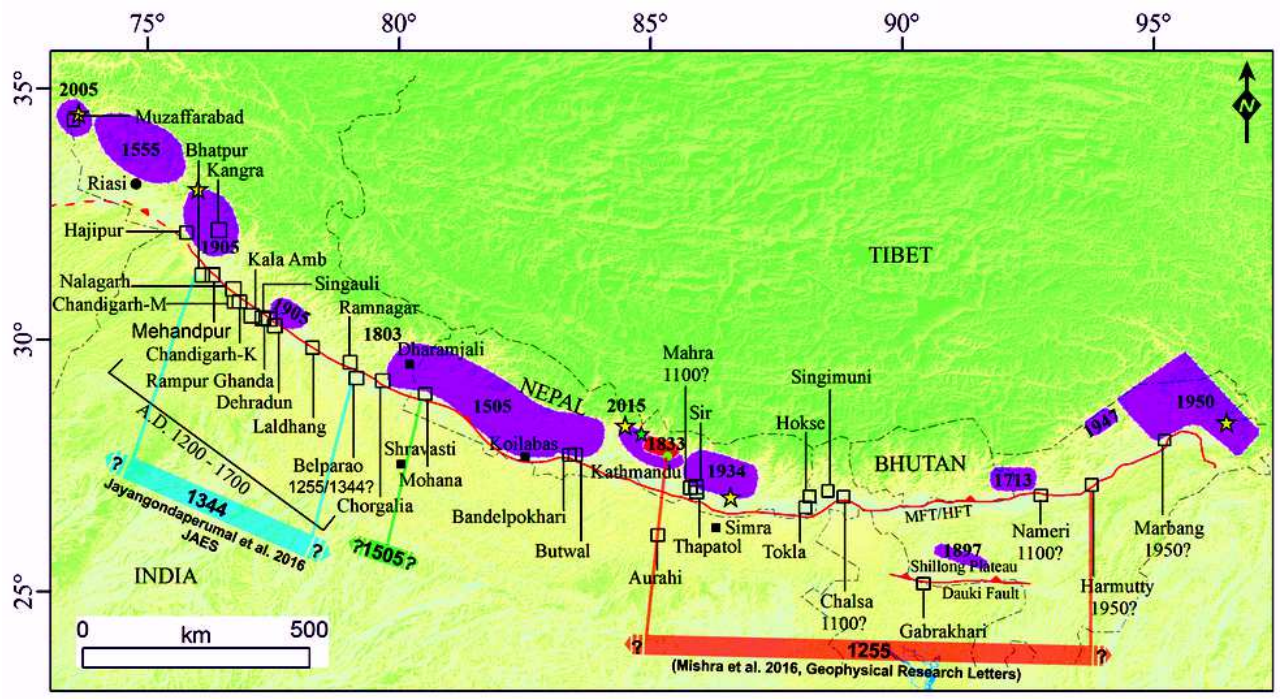

Fig. 2: Simplified SRTM map of Himalaya showing instrumental and historical earthquakes rupture extents along with paleoseismological trench site excavated/studied so far (Open square is connected with thick line). Horizontal colour (orange, blue and green) bars showing surface ruptures extent discovered through trench excavation. Note historical evidences for the A.D. 1255 and A.D. 1344 are well documented in Kathmandu valley, which are in harmony with trenched surface ruptures. In NW Indian Himalaya historical documents and trenched surface rupture events are incompatible. However, archeao-seismological study apparently matches with trench study results that suggest damage event occurred during twelfth-thirteenth century A.D. (Source: Jayangondaperumal)

Time-averaged surface velocities, convergence and extension rates along arc-normal transects in Kumaon, Garhwal and Kashmir-Himachal regions were derived from 13 years of high-precision Global Positioning System (GPS) time series (1995-2008) data at 14 GPS permanent and 42 campaign stations between 29.5°:35°N and 76°:81°E (Jade *et al*., 2014). These measurements reveal that surface horizontal velocities vary significantly from the Higher to Lesser Himalaya and are of the order of 30 to 48 mm/year NE in ITRF 2005 reference frame, and 17 to 2 mm/year SW in an India fixed reference frame indicating that this region is accommodating less than 2 cm/year of the India-Eurasia plate motion (~4 cm/year). Total arc-normal shortening varies between ~10-14 mm/year along different transects of the NW Himalaya between the ITSZ to the north and the Indo-Gangetic foreland to the south indicating high strain accumulation in the Himalayan wedge. This convergence is being accommodated differentially along the arc-normal transects; ~5-10 mm/year in Lesser Himalaya and 3-4 mm/year in Higher Himalaya south of the South Tibetan Detachment. Most of the convergence in the Lesser Himalaya of Garhwal and Kumaon is being accommodated just south of the MCT fault trace, indicating high strain accumulation in this region which is also consistent with high seismic activity. In addition, for the first time an arc-normal extension of ~6 mm/year has also been observed in the Tethyan Himalaya of Kumaon. Inverse modeling of GPS-derived surface deformation rates in Garhwal and Kumaon Himalaya using a single dislocation indicate that the Main Himalayan Thrust (MHT) is locked from the surface to a depth of ~15-20 km over a width of 110 km with associated slip rate of ~16-18 mm/year. Arc-normal rates in the NW Himalaya have a complex deformation pattern involving both convergence and extension, hence rigorous seismotectonic models are necessary to account for this pattern in the Himalaya (Jade *et al*., 2014).

Shah (2013) and Ahmad *et al*. (2012) have mapped major unknown faults and fault segments in Kashmir basin as Kashmir Basin Fault or Balapur Fault, using geomorphological techniques. These faults were interpreted as normal fault by previous workers. Their systematic investigations suggest that strain release along these hinterland faults should be taken up in assessing the seismic hazard.

The rupture related with the most speculated 1905 Kangra earthquake of Mw ~7.8 was discovered in a trench survey across an out-of-sequence fault called, the Kangra Valley Fault (KVF) indicating its active participating in strain release (Malik *et al*., 2015). It invokes a revision of the strain partitioning of 14 mm/yr long-term convergence estimated across the Kangra re-entrant by Thakur *et al*. (2014).

Singh *et al*. (2012) investigated broader epicentral area of the M=7.8, 1905 Kangra earthquake(s) in the NW Himalayan Sub-Himalayan hills between two major re-entrants (Kangra and Dehradun) and intervening Nahan Salient. The first-order topography between the HFT and the MBT shows a marked lateral variation in mean gradient along strike, and is characterized by a very small mean slope angle (~1°) in the re-entrants and higher values (~3°) in the salient regions. These tectonic and topographic features also show a good correspondence with peculiar macroseismic field of the 1905 event(s), which is characterized by two distinct intensity maxima, separated by a distance of ~150 km, and clearly overlapping the two major tectonic re-entrants. Singh *et al*. (2012) assessed the critical taper model to clarify the possible correlations between tectonics, topography and seismicity in the Sub-Himalayan belt, where three possible seismotectonic scenarios are explored in order to constrain their likelihood. They suggested a potential seismic gap corresponding to the Nahan Salient, which may experience an event of significant magnitude in the future.

Darjeeling-Sikkim Himalayan (DSH) seismicity is unique in that it is dominated by moderate thrust and strike-slip earthquakes (Mukul *et al*., 2014). Hypocenters cluster not only near the location of the MHT or the basal decollement of the Himalayan wedge, but also well above and below it. Epicentres cluster over mapped location of the Lesser Himalayan Duplex (LHD), suggesting that both the MHT and the LHD are active structures. Earthquakes below the MHT can be related to strike-slip faulting in the DSH. The 18 September 2011 (Mw 6.9) strike-slip event suggests that this salient is also likely to contain active oblique strike-slip faults. High-precision GPS measurements (1997-2006) indicate that a maximum of ~4 mm/year convergence is being accommodated in the Tista Half-Window or LHD west of the surface

trace of the GTF; the DSH is locked south of 27ºN both east and west of the GTF about 10 km north of the Himalayan mountain front (Mukul *et al*., 2014).

Rajendran and Rajendran (2011) postulated that only earthquakes occurring on faults between the tectonic wedges are able to promote the rupture outwards as coseismic displacements (e.g., 2005 Kashmir earthquake), whereas the rupture propagation for earthquakes occurring on the basal detachment gets hindered by the crustal ramps (e.g., 1905 Kangra, 1934 Bihar) leading to blind events. However, their work was later contested by surface rupture evidences along the HFT in Nepal Himalaya and out-of-sequence KVF in Kangra valley (Malik *et al*., 2015). The preceding paragraphs for the western parts of NW Himalaya highlight the role of out-of-sequence faulting for release of strain energy during earthquakes, implying that a general seismotectonic model in which most of the strain is being released along the MFT as inferred in the central Nepal Himalaya cannot be used for Seismic Hazard Assessment (SHA).

Evidences for great surface rupturing earthquake were observed at Pasighat along the HFT in Arunachal (Jayangondaperumal *et al*., 2011), where a scarp was primarily formed in a single large earthquake post-1011 cal yr BP (Before Present), followed by an earthquake event post-2009 cal yr BP. Withstanding the uncertainty in timing of earthquakes, they documented occurrence of large scarp-forming earthquakes. Possibility of tilting of sediments that occurred post-2009 cal yr B.P. as the result of historical 1950 Assam earthquake cannot be overruled.

In the Bhutan-Himalayan foothills, Kokrajhar District, Assam, Dasgupta *et al*. (2013) mapped a 30 km long east-west trending, south dipping frontal active back thrust in the outboard of MFT. This thrust is active since 16 ka and propagates toward hinterland with a complementary incipient south-facing scarp.

Mugnier *et al*. (2013) documented structural interpretation of great earthquakes for Western, Central and Eastern Himalaya. Their study suggests to an irregular cycle of seismicity, and great/mega earthquakes could occur at any time along the HFT. Further, they suggested A.D. 1344 or 1408 event in Kumaon Himalaya, which has been confirmed by Rajendran *et al*. (2013) through archeo-seismological study of ancient temple monuments in this region. Phillip *et al*. (2012) trenched across the HFT trace in Singhauli village near Kala Amb and recorded two large magnitude events between 29-17 ka and 5.8-2 ka capable of producing 12-16 m and 20-22 m slip.

Kumahara and Jayangondaperumal (2013) have presented new trench results at Bhatpur together with seven previously-excavated trenches between Hajipur and Ramnagar along the HFT. They proposed two scenarios: i) a single event rupture for all sites between A.D. 1200 and A.D. 1630 with a rupture length of at least 450 km and coseismic slip of 9-26 m or ii) two events of lateral extent overlapping at Kala Amb trench site (Black mango tear fault connecting two HFT strands); the latest event occurred between A.D. 1400 to A.D. 1460 in the northwestern extent producing a ~9 m coseismic displacement over a 200 km fault length. The penultimate event occurred between A.D. 1282 and A.D. 1422 across a 230 km fault length and produced coseismic displacements between 16-26 m in the southeastern extent. Yet other two overlapping events (pre-1400 A.D. and another unknown older event) were inferred at Ramnagar trench site in the southeastern extent by applying various geometrical and kinematic tests to faults and folds observed in the trench exposures (Jayangondaperumal *et al*., 2013). Their recent inferences negated a single event mega earthquake scenario proposed previously.

In the same context, Rajendran *et al*. (2015a) have re-excavated a trench 20 m west of 2006 Kumar's *et al*. trench site in Ramnagar. They have inferred two events between A.D. 1050-A.D. 1259 and A.D. 1259-A.D. 1433. Of these events, the penultimate event was loosely correlated either with A.D. 1100 or A.D. 1255, which were reported previously in Nepal. Further they have speculated that the most recent event was ascribed to A.D. 1344, as demonstrated by Jayangonadaperumal *et al*. (2013) in western Nepal and not due to the great A.D. 1505 earthquake, which has been confirmed by Rajendran *et al*. (2013) through archeo-seismological study of ancient temple monuments in Kumaon and Garhwal Himalaya.

Rajendran *et al*. (2015b) have attempted to infer the paleoearthquake event by studying stalagmites

from three limestone caves along major structural discontinuities i.e., MCT, MBT and HFT in Kumaon Himalaya. However, the only discussed results from Dharmaji cave in vicinity of the MCT show the last deformation correlated with the A.D. 1050-A.D. 1259 and A.D. 1259-A.D. 1433 in the previous study by Rajendran *et al*. (2015a) and another event ~1500 year BP. Further from the study of liquefaction features in the Bihar and Uttar Pradesh plains, Rajendran *et al*. (2016) showed record for at least 3 seismic events between 10-19th centuries, reflecting high seismic hazard for Bihar with a recurrence interval of 124±63 years for moderate to large earthquakes.

Pandey and Pandey (2015) have interpreted formation of soft sediment deformation features due to earthquake activity, as recorded in depositional facies of 26-25 ka old fluvio-lacustrine channel-fill deposits of Yamuna River in western Dehra Dun valley.

To test whether an earthquake of Mw 9 could occur within the Himalayan region, Gupta and Gahalaut (2015) reviewed earthquake scenario in the Himalayan region, and concluded that although this possibility could not be entirely rejected, segmentation of the Himalayan belt and distributed deformation along different faults within the belt do not support the prospect of a Mw 9 event. However, a great earthquake of M>8 occurring anywhere in the Himalayan region could cause severe damage and loss of life worth one million as tested from a hypothetical scenario of Mw 8 in Mandi, NW Himalaya.

Parameswaran *et al*. (2015) carried out ground mapping of areas damaged by the 2015 Gorkha twin events (Mw 7.8 and 7.6) where surface rupture remains blind and confined in the hinterland. After studying the 2015 Gorkha earthquake event, Mitra *et al*. (2015) reaffirmed that majority of convergence between India and Tibet is stored as elastic strain energy and is released by brittle failure in earthquakes.

Geometry of the Indian Plate (IP) in the Himalaya

During the period 2011-2015 two magnetotelluric (MT) profiles were run in the NW Himalaya from Roorkee to Gangotri (Miglani *et al*., 2014) and Bijnor-Joshimath-Malari to decipher the geometry of the Indian Plate (IP). Along the Roorkee-Gangotri MT profile, Miglani *et al*. (2014) distinguished the following characteristic features (Fig. 3A):

(i) *Feature-A*: A shallow conductive structure (<50 Ωm) in southern parts within the IGP and SH region with maximum thickness up to 7 km. This zone corresponds to loose sediments of the IGP, and Siwalik Group of rocks of the Miocene and younger ages within the IGP and SH. The resistive zone below these conducting sediments is interpreted as the top of the Indian Plate (IP).

(ii) *Feature-B*: An electrically-high resistive (1000 Ωm) basement representing the subducting Indian Plate (IP). Its southernmost part shows a low resistivity zone, which may be associated with fluid-saturated fractured zone, possibly belonging to the Main Himalayan Thrust (MHT) along which the IP subducts beneath the Himalaya (Miglani *et al*., 2014).

(iii) *Feature-C*: A low resistivity (<10 Ωm) feature beneath the MCT zone as a typical example of mid-crustal conductor, invariably observed in the Himalayan region. This zone exhibits high seismicity and controls more recently recorded earthquake hypocenters (Mahesh *et al*. 2013; see Fig. 5A). Additional earthquake data brought clustering of earthquake hypocenters towards the boundary of conductive-resistive zones. This zone may also be associated with geothermally-anomalous zone having high temperatures, high heat flow and hot springs in the MCT zone. Alternatively, this low resistivity zone can also be interpreted as a partially molten layer. The most likely conductive phase is the fluid, since underthrusting of the Indian crust can ensure continuous recharge of the hanging wall by fluids released during dehydration reactions. The model suggests possible flat-ramp-flat geometry of the MHT (Fig. 3A).

(iv) *Feature-D*: It is an electrically resistive feature below 30 km and may represent an electrical image of subducting crustal part of the Indian Plate.

In summary, it is possible to draw tectonic surface of the MHT as subhorizontal flat up to the MCT, and a ramp and further nearly sub-horizontal

flat surface in the north (Fig. 3A). The MHT geometry, as shown in the model, justifies the clustering of the earthquake locations above the ramp and conducting fluid-saturated fractured region in the MCT zone.

Further southeast along the Bijnor-Joshimath-Malari traverse, Rawat *et al*. (2014) observed about 5 km thick low-angle and NE-dipping intra-crustal high conducting layer (IC-HCL) of very low resistivity across the IGP and the Higher Himalaya with an intervening ramp (Fig. 3B). The following near-surface resistivity distribution is consistent with the exposed lithologies and structural features:

(i) High resistivity (>1000 Ωm) zone corresponding to the dry and compact high-grade metamorphic rocks of the HHC ("L").

(ii) Comparable thin high resistivity blocks between C and D corresponding to the Garhwal and Almora Klippe supporting the geological hypothesis that metamorphic sheets occupying the core regions of these klippe are basically the HHC, which has migrated southward to their present position during the foreland propagating thrusting.

(iii) Subhorizontal to NE-dipping intra-crustal high conducting layer (IC-HCL) of across the IGP and the Higher Himalaya. In extreme south it is located at shallow ~3-5 km depth (A), extending sub-horizontally northeastwards and deepening to ~8 km beneath SH and LH (B to D). With an average thickness of about 5 km, this layer has an average resistivity of 5 Ωm and a conductance of the order of 1000 S. It steepens beneath the MCT to acquire the ramp geometry (Fig. 3B; Rawat *et al*., 2014).

(iv) Confinement of aftershocks of the Chamoli

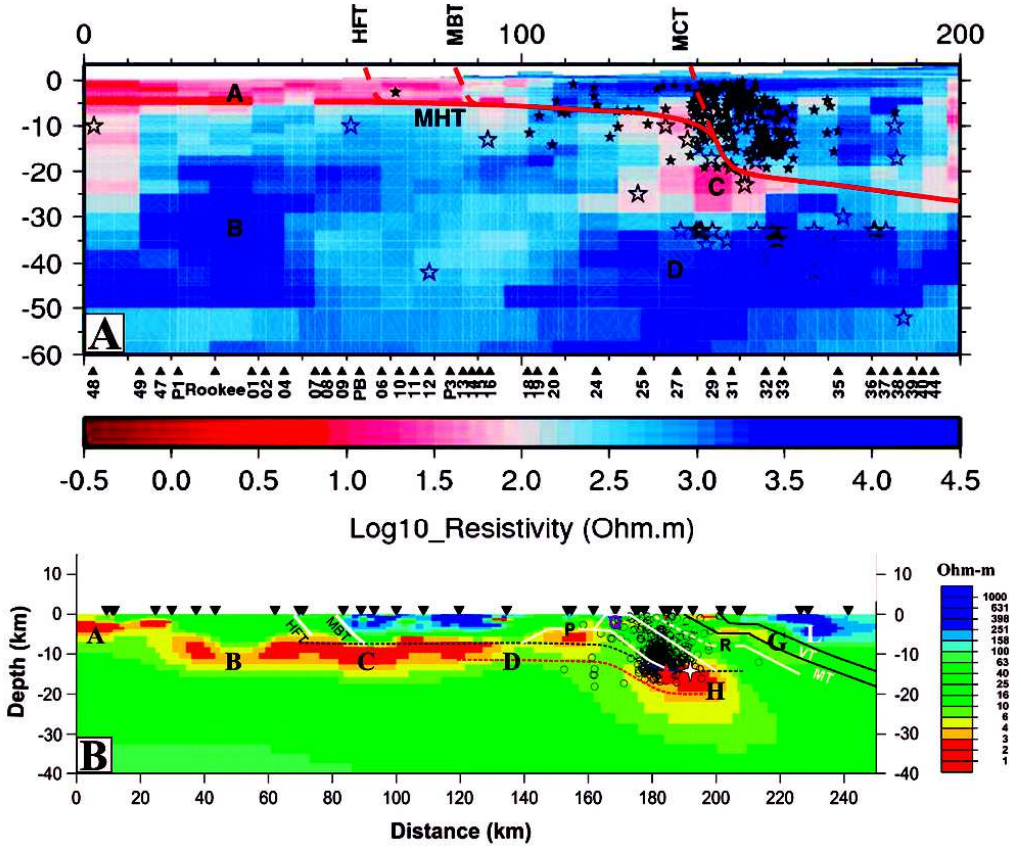

Fig. 3: Magnetotelluric sections of the Garhwal Himalaya. (A) Roorkee-Gangotri profile showing low resistivity (<10 Ωm) zone beneath MCT and cluster of small associated earthquakes. After Miglani *et al*. (2014). (B) Bijnor-Joshimath-Malari section showing low resistivity zone (A-B-C-D-H) and hypocenters of the Chamoli Earthquake. After Rawat *et al*. (2014)

earthquake. These were localized to a narrow pocket rising from depth of the main shock into the overlying duplex. (v) Detection of the MCT zone as a low resistivity zone rising from the depth of fluid filled IC-HCL up to the surface as an example of syntectonic fluid flow.

The whole structure also controls velocities of seismic waves in intra-crustal low velocity layer (IC-LVL) (cf., Caldwell *et al*., 2013). These coincident layers are fluid-saturated which could be the released water from metamorphic reactions or partial melt.

References

Adlakha V, Lang K A, Patel R C, Lal N and Huntington K W (2013b) Rapid long-term erosion in the rain shadow of the Shillong Plateau, Eastern Himalaya *Tectonophysics* **582** 76-83

Adlakha V, Patel R C and Lal N (2013c) Exhumation and its mechanisms: A review of exhumation studies in the Himalaya *Jour Geol India* **81** 481-502

Adlakha V, Patel R C, Lal N, Mehta Y P, Jain A K and Kumar A (2013a) Tectonics and climate interplay: exhumation patterns of the Dhauladhar Range, NW Himalaya *Current Sci* **104** 1551-1559

Agarwal, Amar, Agarwal K K, Bali R, Chandra P and Joshi G (2016) Back-thrusting in Lesser Himalaya: Evidence from magnetic fabric studies in parts of Almora Crystalline zone, Kumaon Lesser Himalaya *Jour Earth System Science*

Agarwal K K and Sharma V K (2011) *Quaternary tilt-block tectonics in parts of Eastern* Kumaon Himalya, India. Zeitschrift für Geomorphologie N.F., v. 55, p. 197-208

Agarwal K K, Chandra P, Ali S N and Jahan N (2012) *Morphometric analysis of the Ladhiya and Lohawati river basins* Kumaon Lesser Himalaya, India Zeitschrift fur Geomorphologie N.F., v. 56, p. 201-224

Agarwal K K, Sharma A, Jahan N, Prakash C and Agarwal A (2011). Occurrence of pseudotachylites in the vicinity of South Almora Thrust zone, Kumaon Lesser Himalaya *Current Sci* **101** 431-434

Ahmad S and Bhat M I (2012) Tectonic geomorphology of the Rambiara basin, SW Kashmir Valley reveals emergent out-of-sequence active fault system *Him Geol* **33** 162-172

Anczkiewicz R, Chakraborty S, Dasgupta S, Mukhopadhyay D K and Kotonik K (2014) Timing, duration and inversion of prograde Barrovian metamorphism constrained by high resolution Lu-Hf garnet dating: A case study from the Sikkim Himalaya, NE India *Earth Planet Sci Letts* **407** 70-81

Banerjee D M (2013) Carbon and sulfur isotope records of Ediacaran carbonates of Lesser Himalaya: implication on oxidative state of the contemporary oceans. 23rd HKT, *Laddakh Himalaya* **5** 21 (Abstract)

Banerjee S, Matin A and Mukul M (2015) Overburden-induced flattening structure in the Himalaya: mechanism and implication *Current Sci* **109** 1814-1820

Bhargava O N (2015) Evolution of the Tethyan and Karewa successions in Kashmir: a synthesis *Jour Palaeont Soc India* **60** 51-72

Bhargava O N and Draganitis E (2015) India Devonian (Himalaya). In Suttner *et al.* 2016 Planet Earth in Deep Times. Schweizerbart Science Publishers, Stuttgart, 119-120

Bhargava O N and Srikantia S V (2014) Geology and age of metamorphism of the Jutogh and Vaikrita Thrust Sheets, Himachal Himalaya *Himalayan Geol* **35** 1-15

Bhargava O N (2011) Early Palaeozoic paleogeography, Basin configuration, Paleoclimate and tectonics in the Indian Plate *Mem Geol Soc India* 78 69-99

Bhargava O N, Frank W and Bertle R (2011a) Late Cambrian deformation in the Lesser Himalaya *Jour Asian Earth Sci* **40** 201-212

Bhargava O N, Kaur G and Deb M (2011b) Paleoproterozoic paleosol in the Lesser Himalaya *Jour Asian Earth Sci* **42** 1371-1380

Bhargava O N, Thöni M and Miller C (2015) Early Palaeozoic garnet in the Jutogh Group, Himachal Himalaya, India: Its regional implications. Abstract. 30th Himalayan-Karakoram-Tibet Workshop, Dehradun, 6-8 October, p. 5-6

Bhatia S B, Bhargava O N, Singh Birendra P and Bagi H (2014) Sequence stratigraphic framework of the Paleogene succession of the Himalayan Foreland Basin: a case study from the Shimla Hills. *Jour Palaeont Soc India* **58** 21-38

Bhattacharyya K and Ahmed F (2016) Role of initial basin width in partitioning total shortening in the Lesser Himalayan fold-thrust belt: Insights from regional balanced cross-sections *Jour Asian Earth Sci* **116** 122-131

Bhattacharyya K and Mitra G (2014) Spatial variations in deformation mechanisms along the Main Central thrust zone: Implications for the evolution of the MCT in the

Darjeeling -Sikkim Himalaya *Jour Asian Earth Sci* **96** 132-147

Bhattacharyya K, Dwivedi H V, Das J P and Damania S (2015a) Structural geometry, microstructural and strain analyses of L-tectonites from Paleoproterozoic orthogneiss: Insights into local transport-parallel constrictional strain in the Sikkim Himalayan fold thrust belt *Jour Asian Earth Sci* **107** 212-231

Bhattacharyya K, Mitra G and Kwon S (2015b) Geometry and kinematics of the Darjeeling-Sikkim Himalaya, India: Implications for the evolution of the Himalayan fold-thrust belt *Jour Asian Earth Sci* **113** 778-796

Caldwell W B, Klemperer S L, Lawrence J F, Rai S S and Ashish (2013) Characterizing the Main Himalayan Thrust in the Garhwal Himalaya, India with receiver function CCP stacking *Earth Planet Sci Lett* **367** 15-27

Dasgupta S, Mazumdar K, Moirangcha L H, Dutta Gupta T and Mukhopadhyay B (2013) Seismic landscape from Sarpang re-entrant, Bhutan Himalaya foredeep, Assam, India: Constraints from Geomorphology and Geology *Tectonophysics* **592** 130-140

De Sarkar S, Mathew G and Pande K (2013a) Arc parallel extension in Higher and Lesser Himalayas, evidence from western Arunachal Himalaya *India Jour Earth Syst Sci* **122** 715-727.

De Sarkar S, Mathew G, Pande K, Chauhan N and Singhvi A K (2013b) Rapid denudation of Higher Himalaya during late Pleistocene, evidence from OSL thermochronology *Geochronometria* **40** 304-310

Faak K, Chakraborty S and Dasgupta S (2012) Petrology and tectonic significance of metabasite slivers in the Lesser and Higher Himalayan domains of Sikkim *India Jour Metam Geol* **30** 599-622

Gaides F, Arianne P -R, Chakraborty S, Dasgupta S and Jones P (2015) Constraining the conditions of Barrovian metamorphism in Sikkim, India: P-T-t paths of garnet crystallization in the Lesser Himalaya *Jour Metam Geol* **33** 23-44

Ghosh N, Basu A R, Bhargava O N, Shukla U K, Ghatak A, Garzione C N and Ahluwalia A D (2014) Catastrophic environmental transition at the Permian-Triassic Neo-Tethyan margin of Gondwanaland: Geochemical, isotopic and sedimentological evidence in the Spiti Valley, India. Gondwana Res., http://dx.doi. org/10. 1016/j.gr. 2015.04.006

Gupta H K and Gahalaut V K (2015) Can an earthquake of Mw? 9 occur in the Himalayan region? *Geol Soc London Spec Publ* **412** 43-53

Jade S, Mukul M, Gaur V K, Kumar K, Shrungeshwar T S, Satyal G S, Kumar R, Dumka Jagannathan S, Ananda M B, Dileep Kumar P and Banerjee S (2014) Contemporary deformation in the Kashmir-Himachal, Garhwal and Kumaon Himalaya: significant insights from 1995-2008 GPS time series *Jour Geodesy* **88** 539-557

Jain A K, Seth P, Shreshtha M, Mukherjee P K and Singh K (2013) Structurally-controlled melt accumulation: Himalayan migmatites and related deformation, Dhauli Ganga Valley, Garhwal Himalaya *Jour Geol Soc India* **82** 313-318

Jain A K, Shreshtha M, Seth P, Kanyal L, Carosi R, Montomoli C, Iaccarino S and Mukherjee P K (2015) The Higher Himalayan Crystallines, Alaknanda - Dhauli Ganga Valleys, Garhwal Himalaya, India. In: (Eds.) Montomoli, C., Carosi, R., Law, R., Singh, S. and Rai, S.M., Geological field trips in the Himalaya, Karakoram and Tibet *Journal of the Virtual Explorer*, *Electronic Edition*, ISSN 1441-8142 **47** paper 8, 1-34

Jayangondaperumal R, Mugnier J L and Dubey A K (2013) Earthquake slip estimation from the scarp geometry of Himalayan Frontal Thrust, western Himalaya: implications for seismic hazard assessment. *Intern Jour Earth Sci* **102** 1937-1955

Jayangondaperumal R, Wesnousky S G and Choudhuri B K (2011) Near-surface expression of early to late Holocene displacement along the northeastern Himalayan frontal thrust at Marbang Korong Creek, Arunachal Pradesh *India Bull Seismol Soc Amer* **101**3060-3066

Kellett D A, Grujic D, Coutand I, Cottle J and Mukul M (2013) The South Tibetan detachment system facilitates ultra rapid cooling of granulite-facies rocks in Sikkim Himalaya *Tectonics* **32** 252-270

Kumahara Y and Jayangondaperumal R (2013) Paleoseismic evidence of a surface rupture along the northwestern Himalayan Frontal Thrust (HFT) *Geomorphology* **180** 47-56

Kundu A, Matin A and Mukul M (2012) Depositional environment and provenance of Middle Siwalik sediments in Tista valley, Darjeeling District, Eastern Himalaya *India Jour Earth Sys Sci* **121** 73-89

Kundu B, Yadav R K, Bali B S, Chowdhury S and Gahalaut V K (2014) Oblique convergence and slip partitioning in the NW Himalaya: implications from GPS measurements *Tectonics* **33** 2013-2024

Lahoti S, Kumud K, Gupta Y and Jain A K (2016) Tectonics of the Chamba Nappe, NW Himalaya and its regional implications *Italian Jour Geosci* **136** doi: 10.3301/

IJG.2015.39

Leech M, Coble M A, Singh S, Guillot S and Jain A K (2014) New U-Pb age and trace element composition of young metamorphic zircon rims from the UHP Tso Morari Complex, NW Himalaya, distinguishes peak from retrograde metamorphism. 2014 GSA Annual Meeting in Vancouver, British Columbia, Paper No. 181-13

Mahesh P, Rai S S, Sivaram K, Paul A, Gupta S, Sarma R and Gaur V K (2013) One dimensional reference velocity model and precise locations of earthquake hypocenters in the Kumaon-Garhwal Himalaya *Bull Seis Soc Amer* doi: 10.1785/0120110328 **103** 328-339

Malik J N, Sahoo S, Satuluri S and Okumura K (2015) Active Fault and paleoseismic studies in Kangra Valley: evidence of surface rupture of a Great Himalayan 1905 Kangra Earthquake (Mw 7.8), Northwest Himalaya *India Bull Seism Soc Amer* **105** 2325-2342, doi: 10.1785/0120140304

Mathew G, De Sarkar S, Pande K, Dutta S, Ali S, Rai A and Netrawali S (2013) Thermal metamorphism of the Arunachal Himalaya, India: Raman thermometry and thermochronological constraints on the tectono-thermal evolution *Int Jour Earth Sci (GeolRundsch)* **102** 1911-1936

McKenzie N R, Hughes N C, Myrow P M, Singh B P, Jiang Q, Planavsky N J, Webb A A G, Colleps C L, Banerjee D M, Deb M and Stockli D F (2015) Constraints on the stratigraphic architecture of the Uttarakhand-Himachal Lesser Himalaya: Implication for the evolution of the North Indian margin. 24th HKT Conference and Field Workshop, Dehradun (Abstract)

Miglani R, Shahrukh M, Israil M, Gupta P K, Varsheney S K and Sokolova E (2014) Geoelectric structure estimated from magnetotelluric data from Uttarakhand Himalaya *India Jour Earth Syst Sci* **123** 907-918

Mitra S, Paul H, Kumar A, Singh S K, Dey S and Powali D (2015) The 25 April 2015 Nepal earthquake and its aftershocks *Current Sci* **108** 1938-1943

Mottram C M, Argles T W, Harris N B W, Parish R R, Horstwood M S A, Warren C J and Gupta S (2014) Tectonic interleaving along the Main Central Thrust, Sikkim Himalaya *Jour Geol Soc London* **171** 255-268

Mugnier J L, Gajurel A, Huyghe P, Jayangondaperumal R, Jouanne F and Upreti B (2013) Structural interpretation of the great earthquakes of the last millennium in the central Himalaya *Earth-Sci Reviews* **127** 30-47

Mukul M, Jade S, Ansari K and Matin A (2014) Seismotectonic implications of strike-slip earthquakes in the Darjeeling-Sikkim Himalaya *Current Sci* **106** 198-210

Myrow P M, Hughes N C, Derry L A, McKenzie N R, Jiang G, Webb A A G, Banerjee D M, Paulson T S and Singh B P (2015) Neogene marine isotopic evolution and the erosion of Lesser Himalayan Strata: Implication for Cenozoic tectonic history *Earth Planet Sci Lettr* **417** 132-150

Nandini P and Thakur S S (2011) Metamorphic evolution of the Lesser Himalayan Crystalline Sequence, Siyom Valley, NE Himalaya *India Jour Asian Earth Sci* **40** 1089-1100

Pandey A K and Pandey P (2015) Soft Sediment Deformation structures in late Quaternary abandoned channel fill deposit of Yamuna River in NW Sub Himalaya *India Current Sci* **108** 1717-1725

Pandey A K, Pandey P, Singh G D and Juyal N (2014) Climate footprints in the Late Quaternary-Holocene landforms of Dun Valley, NW Himalaya, India. In: Spec. Section: Science of the Himalaya *Curr Sci* **106** 245-253

Pandey S and Parcha S K (2013) Systematics, Biometry of the species *Opsidiscus* from the Middle Cambrian succession of the Spiti Basin *India Jour Geol Soc India* **82** 330-338

Parameswaran R M, Natarajan T, Rajendran K, Rajendran C P, Mallick R, Wood M and Lekhak H C (2015) Seismotectonics of the April-May 2015 Nepal earthquakes: An assessment based on the aftershock patterns, surface effects and deformational characteristics *Jour Asian Earth Sci* **111** 161-174

Parcha S K and Pandey S (2011a) Devonian Ichnofossils from the Farakah Muth Section of the Pin Valley, Spiti Himalaya *Jour Geol Soc India* **78** 263-270

Parcha S K and Pandey S (2011b) Ichnofossils and their significance in the Cambrian successions of the Parahio Valley in the Spiti Basin, Tethys Himalaya *India Jour Asian Earth Sci* **42** 1097-1116

Patel R C, Adlakha V, Lal N, Singh P and Kumar Y (2011) Spatiotemporal variation in exhumation of the Crystallines in the NW-Himalaya, India: Constraints from Fission Track dating analysis *Tectonophysics* **504** 1-13

Patel R C, Singh P and Lal N (2015) Thrusting and back-thrusting as post-emplacement kinematics of the Almora klippe: Insights from Low-temperature thermochronology *Tectonophysics* **653** 41-51

Philip G, Bhakuni S S and Suresh N (2012) Late Pleistocene and Holocene large magnitude earthquakes along Himalayan Frontal Thrust in the Central Seismic Gap in NW Himalaya, Kala Amb, India *Tectonophysics* **580** 162-177

Rajendran C P, John B, Rajendran K and Sanwal J (2016) Liquefaction record of the great 1934 earthquake predecessors from the north Bihar alluvial plains of India *Jour Seis* DOI: 10.1007/s10950-016-9554-z

Rajendran C P, John B and Rajendran K (2015a) Medieval pulse of great earthquakes in the central Himalaya: Viewing past activities on the frontal thrust *Jour Geophy Res: Solid Earth* **120** 1623-1641

Rajendran C P, Rajendran K, Sanwal J and Sandiford M (2013) Archaeological and historical database on the medieval earthquakes of the central Himalaya: ambiguities and inferences *Seis Res Letts* **84** 1-13 Doi: 10.1785/0229130077

Rajendran C P, Sanwal J, Morell K D, Sandiford M, Kotlia B S, Hellstrom J and Rajendran K (2015b) Stalagmite growth perturbations from the Kumaon Himalaya as potential earthquake recorders *Jour Seis* DOI 10.1007/s10950-015-9545-5

Rajendran K and Rajendran C P (2011) Revisiting the earthquake sources in the Himalaya: Perspectives on past seismicity *Tectonophysics* **504** 75-88

Rao D R, Sharma R, Patel R C and Bhakuni S S (2014) Metamorphism and P-T estimates of the Higher Himalayan Crystallines (HHC) of Kaliganga Valley, NE Kumaon Himalaya *India Him Geol* **35** 171-181

Rawat G, Arora B R and Gupta P K (2014) Electrical resistivity cross-section across the Garhwal Himalaya: Proxy to fluid-seismicity linkage *Tectonophysics* **637** 68-79

Rubatto D, Chakraborty S and Dasgupta S (2013) Time scales of crustal melting in the Higher Himalayan Crystallines (Sikkim, Eastern Himalaya) inferred from trace element constrained monazite and zircon chronology *Contrib Miner Petrol* **165** 349-372

Sen K, Dubey A K, Tripathi K and Pfander J A (2012). Composite mesoscopic and magnetic fabrics of the Paleoproterozoic Wangtu Gneissic Complex, Himachal Himalaya, India: Implications for ductile deformation and superposed folding of the Himalayan basement rocks *Jour Geodyn* **61** 81-93

Sen K, Tripathi K and Dubey A K (2013) Is the North Indian continental margin a Palaeo-Proterozoic magmatic arc? Insights from magnetomineralogy and geochemistry of the Wangtu Gneissic Complex, Himachal Lesser Himalaya *Current Sci* **104** 1-8

Shah A A (2013) Earthquake geology of Kashmir Basin and its implications for future large earthquakes *Inter Jour Earth Sci* **102** 1957-1966

Shreshtha M, Jain A K and Singh S (2015) Shear sense analysis of the Higher Himalayan Crystalline Belt and tectonics of the South Tibetan Detachment System, Alaknanda-Dhauli Ganga valleys, Uttarakhand Himalaya *Current Sci* **108** 1107-1118

Singh S (2014) *Pan-African magmatism and Himalayan collisional tectonism* 29th HKT Workshop-Lucca 2-4 September 2014, 151

Singh Birendra P, Virmani N, Bhargava O N, Negi R S, Kishore N. and Gill A (2016) Trilobite fauna of basal Cambrian Series 3 (Stage 5) from the Parahio Valley, Northwest Himalaya, India and its biostrtigrapic significance *Annales de paléontologie* (in press)

Singh Birendra P., Bhargava O N, Juyal K P, Negi R S, Virmani N, Sharma C A and Gill A (2015) Skeletal microfauna from the Cambrian Series 2 (Stage 4) Kunzum La Formation, Parahio valley, Spiti region (Tethyan Himalaya), India *Current Sci* **109** 1-5

Singh Birendra P (2013) AdditionalLate Middle Cambrian Trilobites from the Karsha Formation (Haimanta Group) Zanskar Region of Zanskar-Spiti Basin, Northwest India *Jour Geol Soc India* **81** 361-368

Singh Birendra P, Virmani N, Bhargava O N, Kishore N. and Gill A (2014) *Yuehsienszella* (Cambrian series 2) trilobite from the parahio valley, spiti region (Zanskar-Spiti sub-basin), India and its biostratigraphic significance *Jour Palaent Soc India* **59** 81-88

Singh K (2012) Opposite vergent synclines on the flanks of a large-scale box fold in the Chamba-Lahaul region, northwest Himalaya *India Intern Jour Earth Sci* **101** 997-1008

Singh P, Patel R C and Lal N (2012) Plio-Plistocene in-sequence thrust propagation along the Main Central Thrust zone (Kumaon-Garhwal Himalaya, India): New thermo-chronological data *Tectonophysics* **574-575** 193-203

Singh Preeti, Pant N C, Saikia A and Kundu A (2013) The role of amphiboles in the metamorphic evolution of the UHP rocks: a case study from the Tso Morari Complex, northwest Himalayas *Int Jour Earth Sci* (Geol Rundsch), v. 102, p. 2137-2152. DOI 10.1007/s00531-013-0920-6

Singh S, Awasthi A K, Parkash B and Kumar S (2013) Tectonics or climate: What drove the Miocene global expansion of C4 grasslands? *Int Jour Earth Sci (Geol. Rundsch.)* **102** 2019-2031

Singh T, Awasthi A K and Caputo R (2012) The sub-Himalayan fold-thrust belt in the 1905 Kangra earthquake zone: A critical taper model perspective for seismic hazard analysis *Tectonics* **31** TC6002, doi:10.1029/2012TC003120

Sorcar N, Hoffe U, Dasgupta S and Chakraborty S (2014) High temperature cooling histories of migmatites from the High Himalayan Crystallines in Sikkim, India - rapid cooling unrelated to exhumation *Contrib Miner Petrol* **167** 1-34

Spencer C J, Harris R A, Sachan H K and Saxena A (2011) Depositional provenance of the Greater Himalayan Sequence, Garhwal Himalaya, India: Implications for

tectonic setting *Jour Asian Earth Sci* **41** 344-354

Srivastava G S, Kulshrestha and Agarwal K K (2012) Morphometric evidences of neotectonic block movement in Yamuna Tear Zone of Outer Himalaya, India *Zeitschrift für Geomorphologie NF* **57** 471-484

Srivastava P, Patel S, Singh N, Jamir T, Kumar N, Aruche M and Patel R C (2013) Early Oligocene paleosols of the Dagshai Formation, India: A record of the oldest tropical weathering in the Himalayan foreland *Sediment Geol* **294** 142-156

Srivastava R K (2013) Geochemistry of Proterozoic granitoids exposed between Dirang and Tawang, western Arunachal Himalaya, north-eastern India: petrogenetic and tectonic significance *Int Jour Earth Sci (Geol Rundsch)* **102** 2043-2060

Tarhan L G, Hughes N C, Myrow P M, Bhargava O N, Ahluwalia A D and Kudryavtsev A B (2014) Precambrian-Cambrian boundary interval occurrence and form of the enigmatic tubular body fossil *Shaanxilithes ningoiangesis* from the Lesser Himalaya of India *Palaeontology* **57** 283-298

Thakur S S and Patel S C (2012) Mafic and pelitic xenoliths in the Kinnaur Kailash Granite, Baspa river valley, NW Himalaya: evidence of pre-Himalayan granulite metamorphism followed by cooling event *Jour Asian Earth Sci* **56** 105-117

Thakur S S (2014) Retrograde corona texture in pre-Himalayan metamorphic mafic xenoliths, Sutlej valley, NW Himalaya: Implication on rare occurrence of high-grade rocks in the Himalaya *Jour Asian Earth Sci* **88** 41-49

Thakur S S, Patel S C and Singh A K (2015) A *P–T* pseudosection modelling approach to understand metamorphic evolution of the Main Central Thrust Zone in the Alaknanda valley, NW Himalaya *Contrib Mineral Petrol* **170** DOI 10.1007/s00410-015-1159-y

Thakur V C and Jayangondaperumal (2015) Seismogenic active fault zone between 2005 Kashmir and 1905 Kangra earthquake meizoseismal regions and earthquake hazard in eastern Kashmir seismic gap *Current Sci* **109** 610-617

Thakur V C, Joshi M, Sahoo D, Suresh N, Jayangondapermal R and Singh A (2014) Partitioning of convergence in Northwest Sub-Himalaya: estimation of late Quaternary uplift and convergence rates across the Kangra reentrant, North India *Inter Jour Earth Sci* **103** 1037-1056

Tiwari M, Parcha S K, Shukla R and Joshi H, 2013. Ichnology of the Early Cambrian Tal Group, Mussoorie Syncline, Lesser Himalaya *India Jour Earth Syst Sci* **122** 1467-1475

Tripathi K, Sen K and Dubey A K (2012) Modification of fabric in pre-Himalayan granitic rocks by post-emplacement ductile deformation: insights from microstructures, AMS, and U-Pb geochronology of the Paleozoic Kinnaur Kailash Granite and associated Cenozoic leucogranites of the South Tibetan Detachment zone, Himachal High Himalaya *Int Jour Earth Sci (Geol Rundsch)* **101** 761-772 DOI 10.1007/s00531-011-0657-z

Upadhyay R and Parcha S K (2012) Ichnofossils from the Jadhganga (Nelang) valley, Uttarakashi district, Garhwal Tethys Himalaya, India *Himalayan Geol* **33** 83-88

Vassallo R, Mugnier J L, Vignon V, Malik M A, Jayangondaperumal R, Srivastava P and Carcaillet J (2015) Distribution of the Late-Quaternary deformation in Northwestern Himalaya *Earth Planet Sci Letts* **411** 241-252

Verma A K and Bhattacharya A R (2011) Reorientation of lineation in central crystalline zone, Munsiari-Milam area of the Kumaon Greater Himalaya *Jour Earth Sys Sci* **120** 449-458

Virmani N Singh, Birendra P and Singh Gill A (2015a) Integrated Litho-ichnofacies and ichnofabric analysis of the lowermost part of the Kunzam La Formation along the Khemangar *khad* and the Parahio Valley sections, Spiti Region (Zanskar-Spiti-Kinnaur Basin), Northwest Himalayas, India *Jour Geol Soc India* **85** 557-566

Virmani N Singh, Birendra P Singh, Bhargava O N, Kishore N and Gill A (2015b) Biostratigraphy of the Cambrian succession of the Parahio Valley, Spiti region, Northwest Himalaya. 30th Himalaya-Karakoram-Tibet Workshop, Dehradun, 6-8 October, 86-87 (abstract)

Wiedenbeck M, Goswami J N and Virdi N S (2014) Single Zircon $^{207}Pb/^{206}Pb$ ages from the Garhwal Himalaya (India): Evidence for Paleoproterozoic magmatic activity in the Lesser and Higher Himalaya *Himalayan Geol* **35** l6-2l

Williams J C, Basu A R, Bhargava O N, Ahluwalia A D and Hannigan R E (2012) Resolving original signatures from a sea of overprint-The geochemistry of the Gungri Shale (Upper Permian, Spiti Valley, India) *Chemical Geol* doi:10.1016/j. chemgeo.2012.01.020.